**MULLARD LIMITED**
Mullard House
Torrington Place
London, W.C.1

## CONTENTS

Automatic Magnetiser and Flux-setter for D.C. Permanent Magnet Motors 186–189

Protection against Flashover in Television Picture Tubes 190–192

C.R.T. Grid Drive Circuit using D.C. Restoration of the Unblanking Signal 193–202

Transistor Video Amplifier Design for Monochrome TV Receivers 203–208

**VOL. 10 No. 96 NOVEMBER 1968**

---

# Mullard Technical Communications

VOLUME 10 NUMBER 96 November 1968

**Mullard** Technical Communications

VOLUME 10 NUMBER 96 November 1968

**Contents**

Automatic Magnetiser and Flux-setter for D.C. Permanent Magnet Motors *J. Catherall* 186

Protection against Flashover in Television Picture Tubes *A. Ciuciura* 190

C.R.T. Grid Drive Circuit using D.C. Restoration of the Unblanking Signal *G. W. Broekema* 193

Transistor Video Amplifier Design for Monochrome TV Receivers *M. C. Gander* 203

---

*Mullard Technical Communications* contains information on the performance or application of Mullard products such as semiconductor devices, integrated circuits, electronic valves and tubes, and electrical and magnetic components. It is issued free-of-charge to equipment designers, research organisations, reference libraries, and educational establishments. Applications to be added to the circulation list should be made under an official letter head to Central Technical Services.

Abstracts, or references to an article, should mention both the source, *Mullard Technical Communications*, and the authors. Requests for republication or translation should be made to the Editor in writing.

All articles in *Mullard Technical Communications* are indexed in *British Technology Index*. Abstracts appear in *Current Papers in Physics, Electrotechnology, and Control*.

The issue of the information contained in this publication does not imply any authority or licence for the utilisation of any patented feature.

'Mullard' is the trade mark of Mullard Limited and is registered in most of the principal countries of the world.

Editor: F. A. Sowan
Assistant Editors: E. G. Evans A. Perry

*Published by*
Central Technical Services
Mullard Limited, Mullard House, Torrington Place, London, W.C.1
Telephone: 01-580 6633 Telex: 264341

© Mullard Limited, 1968

Made and Printed in England by
WIGHTMAN AND COMPANY LIMITED, 1/3 BRIXTON ROAD, LONDON, S.W.9

# Automatic Magnetiser and Flux-setter for D.C. Permanent Magnet Motors

J. Catherall
Mullard Magnetic Components, Crossens

*Permanent magnet d.c. motors are found to have different characteristics when tested after production. Performance can be standardised by the measurement and adjustment of the field strength of each motor. The process described in this article can be used before or after final assembly, dependent upon whether the armature can conveniently be driven mechanically or not.*

*Motor speed is adjusted to a specific value by the magnetic saturation of the field pole pieces, and then by demagnetisation to a standard value by controlled pulses of current. All motors then have the same value of magnetic flux.*

*The equipment described performs the magnetisation, measurement, and demagnetisation automatically, accurately, and fast.*

## INTRODUCTION

An earlier article (Ref. 1) described a method of equalising the performance of small permanent magnet d.c. motors after manufacture, by adjusting the field to control the no-load speed. Partial demagnetisation of the field magnet segments was achieved by pulsing the armature current of the motor, using very sensitive equipment. The final specification was determined by the weakest magnets, which did not need adjustment.

The present article describes an alternative method. The pole piece segments are first saturated, and then demagnetised to a standard value of magnetic flux. These functions can be performed before or after final assembly, automatically, accurately and fast.

## PERMANENT MAGNET D.C. MOTORS

Improved manufacturing techniques have made available ceramic permanent magnets designed for use in d.c. motors. The magnets are in the form of segments, the preferred direction of magnetisation produced in the manufacturing process being radial. They have an energy product in excess of $10^4$ joules/m$^3$ ($2{\cdot}5 \times 10^6$ gauss-oersteds), and a high value of the coercive force necessary to prevent demagnetisation by armature reaction.

The structure of motors using these magnets is shown in Fig. 1. The steel tube containing the magnets may form the case of the motor, and then acts as a return path for the magnetic flux.

The characteristics of the motor, in particular the running speed under no-load conditions, are governed by the number of turns and the resistance of the armature winding, the friction of the bearings and brushes, and the flux produced by the field magnets, the latter normally being the largest variable. It is necessary to control the torque/speed characteristics of the motor within certain limits. This is conveniently done by adjusting the magnetic field to control the no-load speed. The necessary limits will be determined by the application of the motor. The method of adjustment described is capable of working to within close limits.

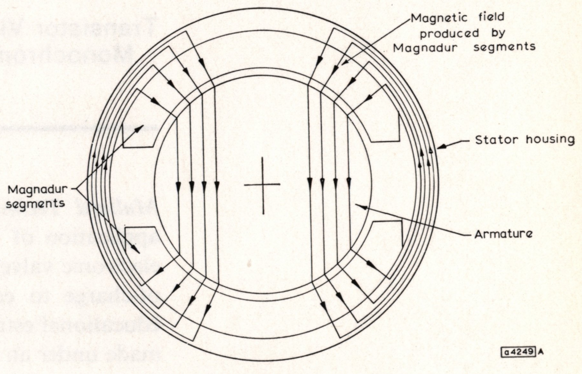

Fig. 1—Motor assembly

When the motors are magnetised, some may have a total flux 20% above the minimum value. Variations in magnetic properties, size of segments, and housing account for this. To produce standard motors, having similar no-load characteristics, the magnetic flux must be measured and then brought to a standard value by demagnetisation.

## OPERATING PRINCIPLES

The magnetic flux in a motor assembly can be measured in one of two ways. If the motor can be driven easily as a generator, the generated voltage at a particular speed can be taken as a measure of total flux. If this method is used the motor can be completely assembled before magnetising. If it is not possible to drive the motor armature, the motor housing with the magnet segments installed in it is magnetised. A Hall probe is then used to measure the flux.

Fig. 2 shows a typical yoke into which the motor housing is fitted. Inside the yoke are pole pieces and field windings ($L_1$). To these field windings are fed demagnetising pulses of gradually increasing amplitude. The effect of this is to reduce the total flux of the motor magnet segments to a standard value. Fig. 3 illustrates this effect on a demagnetising curve.

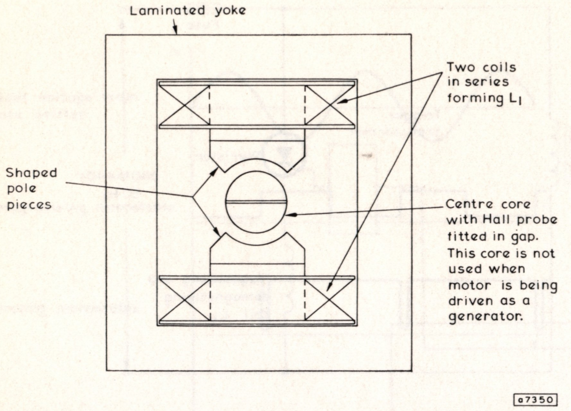
Laminated yoke
Two coils in series forming L1
Shaped pole pieces
Centre core with Hall probe fitted in gap. This core is not used when motor is being driven as a generator.
a7350

Fig. 2—Magnetising/demagnetising yoke for adjusting field strength

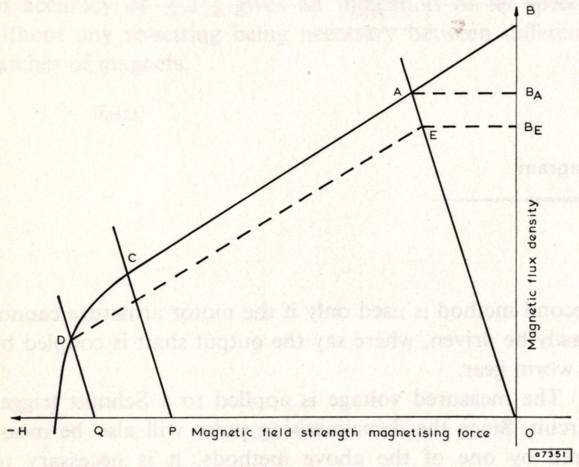

Fig. 3—Demagnetisation curve of magnetic material

OA represents the working line of the motor being treated. The application of a demagnetising pulse moves the working line to the left. When the working line has moved to PC and then returned to OA the flux in the motor will be unchanged, as the flux density recoils from C back to A. However, when the working line OA moves to QD, it intersects the B/H curve beyond the knee of the curve, and when the working line returns to OA the flux density recoils from point D to point E, and the flux density will be reduced from $B_A$ to $B_E$.

Fig. 4 shows an enlarged view of the steep portion, at the knee of the curve. When the demagnetising pulse moves the working line OA to PC the flux will recoil and give a flux density of $B_C$. If a second pulse of slightly greater amplitude is then applied, the working line moves to QD and the flux will recoil to give a flux density of $B_D$.

Owing to the steepness of the demagnetising curve and the working line of the motor, the reduction in flux will be quite large for a small increase in demagnetising current. This indicates that the increase in amplitude between successive pulses needs to be kept quite low if a close tolerance of total flux is required.

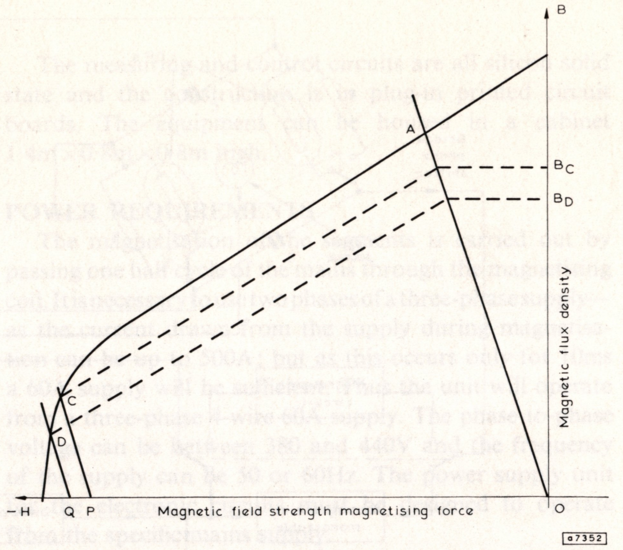

Fig. 4—Enlarged view of the steep portion of the knee of the curve

It can also be seen that it is not necessary for the pulses to start from a very low level. In fact the first pulse can have a value that just fails to reduce the total flux of segments having a minimum coercive force. However, when a motor having segments with a higher coercive force is magnetised this will require a large number of pulses before any reduction in flux occurs. This is shown in Fig. 5. For an acceptable production speed it will be necessary for the pulses to occur at a high repetition frequency.

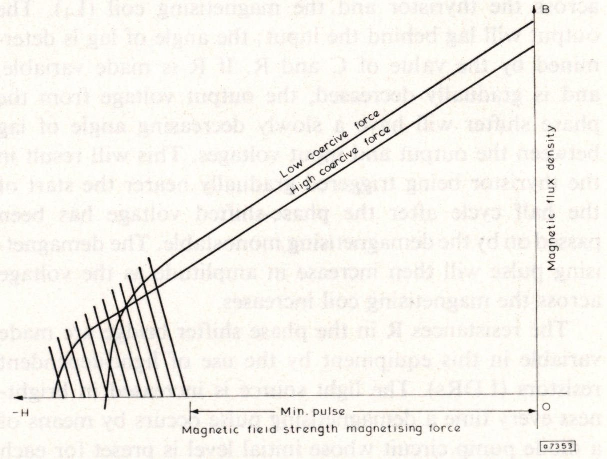

Fig. 5—Number of pulses against coercive force

The demagnetising pulses are obtained from alternate half cycles of the mains (50 pulses/second). The time available in the other half cycles is used to measure the flux. The magnitude of the initial pulse can be controlled and the difference between successive demagnetising pulses can also be altered.

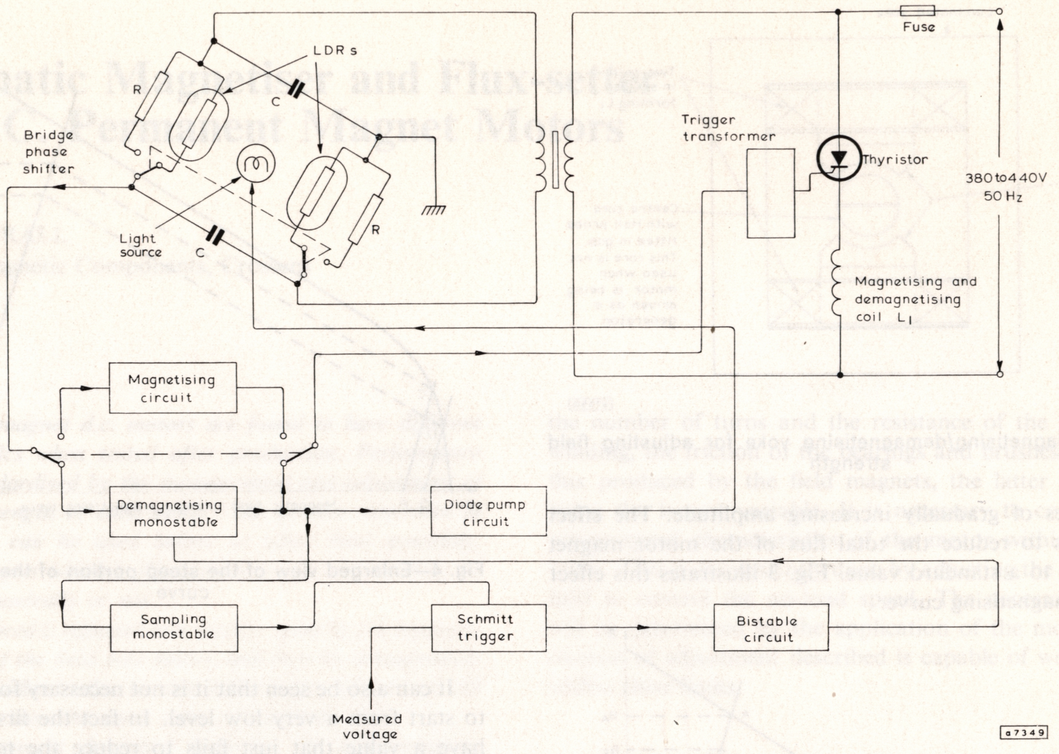

Fig. 6—Block diagram

## CIRCUIT DESCRIPTION

The block diagram of the equipment is shown in Fig. 6. All switches are in the 'Demagnetise' position. The input to the bridge phase shifter will be in phase with the voltage across the thyristor and the magnetising coil ($L_1$). The output will lag behind the input; the angle of lag is determined by the value of C and R. If R is made variable, and is gradually decreased, the output voltage from the phase shifter will have a slowly decreasing angle of lag between the output and input voltages. This will result in the thyristor being triggered gradually nearer the start of the half cycle after the phase-shifted voltage has been passed on by the demagnetising monostable. The demagnetising pulse will then increase in amplitude as the voltage across the magnetising coil increases.

The resistances R in the phase shifter bridge are made variable in this equipment by the use of light-dependent resistors (LDRs). The light source is increased in brightness every time a demagnetising pulse occurs by means of a diode pump circuit whose initial level is preset for each production run.

## MEASUREMENT AND FLUX SETTING

Measurement of the flux can be done in two ways. If it is possible to drive the motor armature mechanically then the whole assembly can be operated as a generator. The second method is to use a Hall probe to measure the flux of the field segments within a motor housing before the insertion of the armature. The output voltage from the Hall probe is amplified by a d.c. amplifier. This second method is used only if the motor armature cannot easily be driven, where say the output shaft is coupled by a worm gear.

The measured voltage is applied to a Schmitt trigger circuit. Since the demagnetising pulse will also be measured by one of the above methods, it is necessary to inhibit the Schmitt trigger by taking an output from the sampling monostable circuit, which allows the Schmitt trigger to sample the measured voltage for about 2ms after the flux has recovered from the demagnetising pulse.

When the measured voltage has fallen to the required value the Schmitt trigger will operate during the sampling period, causing the bistable circuit to switch off the output from the demagnetising monostable. The waveforms at various points are shown in Figs. 7 and 8.

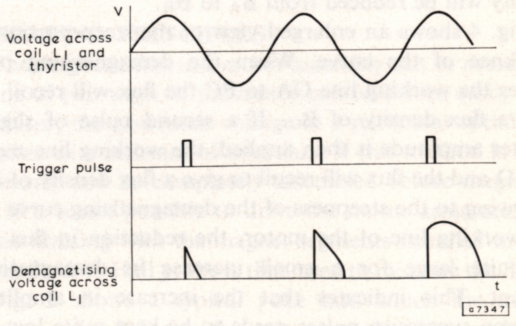

Fig. 7—Pulses against time

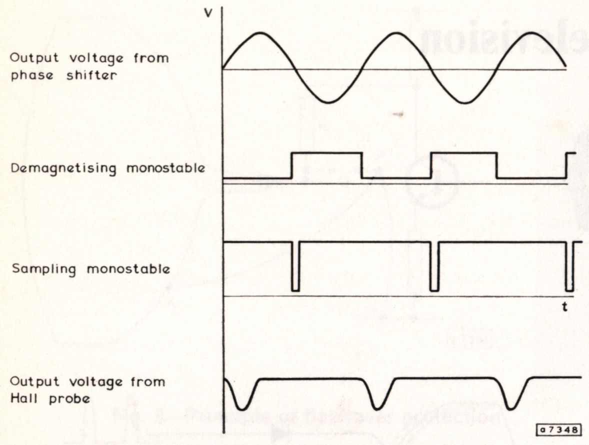

Fig. 8—Waveforms at various points against time

The equipment is capable of producing a standardised total flux of ±1%. An operating time of 5 seconds with an accuracy of ±2% gives an indication of its speed, without any re-setting being necessary between different batches of magnets.

The measuring and control circuits are all silicon solid state and the construction is in plug-in printed circuit boards. The equipment can be housed in a cabinet 1·4m × 0·8m × 0·8m high.

## POWER REQUIREMENTS

The magnetisation of the segments is carried out by passing one half cycle of the mains through the magnetising coil. It is necessary to use two phases of a three-phase supply—as the current drawn from the supply during magnetisation can be up to 500A; but as this occurs only for 10ms a 60A supply will be sufficient. Thus the unit will operate from a three-phase 4-wire 60A supply. The phase-to-phase voltage can be between 380 and 440V and the frequency of the supply can be 50 or 60Hz. The power supply unit for the electronic circuits must be designed to operate from the specific mains supply.

## REFERENCES

1. Catherall, J. 'Equalising the Performances of Small Permanent Magnet D.C. Motors', **Mullard Technical Communications**, Vol. 8, No. 78, November 1965, pp. 236 to 238.

# Protection against Flashover in Television Picture Tubes

A. Ciuciura
**Mullard Central Application Laboratory**

*A method of protecting television receiver circuits against flashover in the picture tube is briefly described. The method uses spark gaps, resistors and flashover bypass connections. Measures to be taken against possible overloading of the e.h.t. supply during the recharging of the e.h.t. capacitor are indicated, and a procedure for testing receivers in respect of flashover is given.*

## MECHANISM AND CONSEQUENCES OF FLASHOVER

Picture tubes, in common with other high-vacuum devices, are prone to internal flashover. There is no generally agreed theory which explains the mechanism producing the high temperatures required for generating the vapour in which the arc is formed. It is likely that, under the influence of electrostatic forces, minute particles are detached and transported across the interelectrode gaps; the energy released on impact may set off the chain of events leading to formation of the arc. The random occurrence of flashover discharges and a return to normal operation after only one discharge seem to support this theory.

Flashover inside a picture tube may occur in several places: directly between electrodes of the gun structure, along the supporting rods, and along the walls of the tube neck. A disturbance originating in this manner reaches the pins on the base of the tube. Some pins receive more discharges than others but, within the life of a tube, each pin will be subjected to flashover. With modern tubes, the number of discharges is sufficiently low to pass unnoticed by viewers; but the problem is of vital importance to circuit designers.

A sketch of a picture tube and some of its supplies is shown in Fig. 1, and a simplified equivalent circuit in Fig. 2. This can be divided into two parts:

a) charging circuit, consisting of e.h.t. supply E, of internal impedance $R_i$, and picture tube capacitance C;

b) discharging circuit, consisting of capacitance C, total inductance L, total resistance R, and a gap g.

A flashover arc closes the gap, and the energy stored in the capacitance is released. Resulting currents may reach a peak value of hundreds of amperes, and the peak voltages may be anything between half and full e.h.t. value.

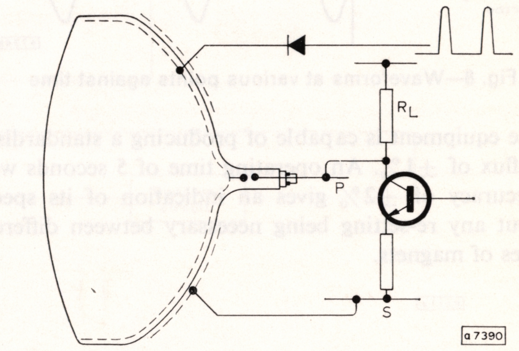

Fig. 1—Basic installation

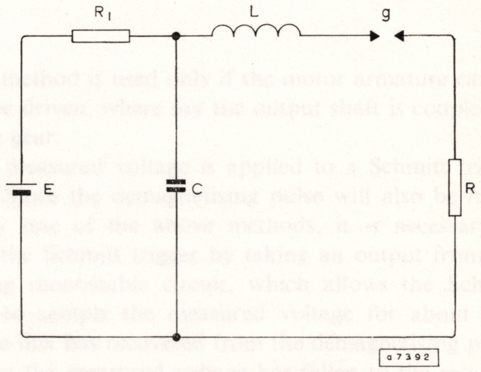

Fig. 2—Simplified equivalent circuit

As a result of flashover, high-energy transients are generated which primarily affect circuits with direct connections to the tube base. A further consequence is the discharge of the capacitor in the e.h.t. supply. While the voltage on the capacitor is recovering, the e.h.t. supply is subjected to considerable overloads.

## PRINCIPLES OF FLASHOVER PROTECTION

A transistor connected to a picture tube as shown in Fig. 1 will form by far the largest part of the total resistance in the discharge circuit. Voltages and currents produced by a flashover will greatly exceed the capabilities of the transistor and failure is inevitable.

An effective method of protection is shown in Fig. 3. (Every electrode should be protected, but for the sake of simplicity, only one pin is shown.) Resistors R and spark-gaps G should be mounted close to the tube socket; all spark-gaps should be returned to the point P.

The circuit possesses three main features, which are discussed below.

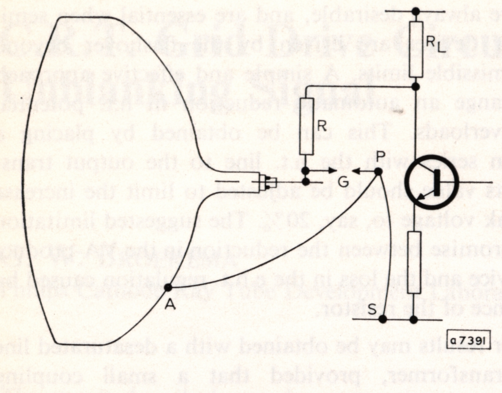

Fig. 3—Principle of flashover protection

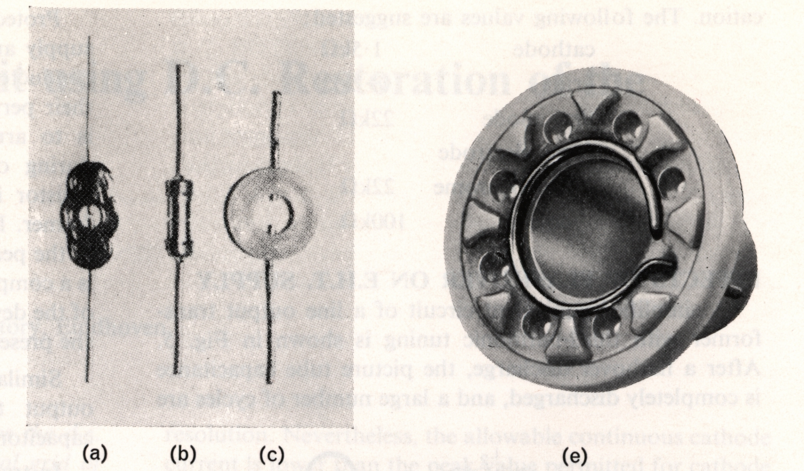

### Flashover bypass path

The flashover bypass path consists of the connection AP between the aquadag coating and the tube base, and the spark-gap G. The spark-gap is operative only during flashover; its object is to conduct discharge currents to the connection AP and thence to the aquadag, thus bypassing receiver circuits.

### Resistor R

Resistor R is connected in series with the supply leads to the pin. In the initial stage of flashover, current flowing through R creates a large potential difference which is necessary to ensure fast breakdown of the spark-gap. At the same time, it limits the current flowing into the transistor, and forms a low-pass filter with any capacitance on the transistor side. Finally, it isolates the receiver circuits from the short circuit produced by the spark-gap.

### Connection SP

The connection SP, by being taken to the tube base instead of to the aquadag directly, eliminates large voltages developed across the flashover bypass AP from receiver circuitry. It also removes any possibility of interaction between the spark-gaps and allows a single connection from the tube base to the aquadag to be used.

The presence of high voltages across connection AP calls for good insulation between the aquadag and the rest of the receiver. Similarly, large currents flowing in the connection require a carefully executed contact to the aquadag.

### Other features

Other relevant and significant stores of energy are the capacitances between the mounting band and deflection coils and the internal conductive coating of the picture tube. Their effects can be minimised by providing direct conduction paths to the aquadag.

A fraction of the flashover current is injected into the chassis via the connecting leads to the tube base; some currents are induced in the chassis through a small capacitance between the chassis and the aquadag. The resulting potential differences can cause difficulties, especially when remotely placed circuits are interconnected, as with an a.g.c. system, for example. Carefully engineered connections and additional decouplings can furnish a sufficient degree of protection.

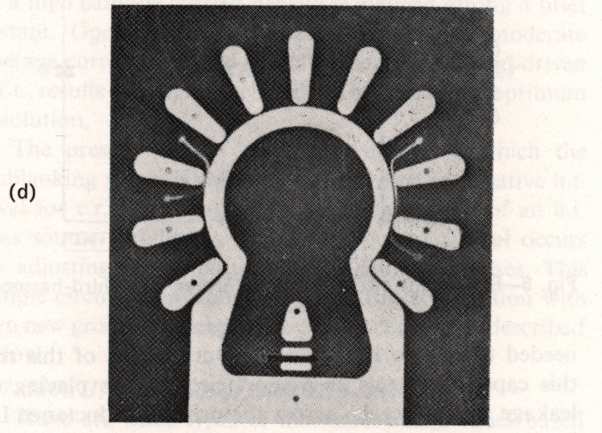

Fig. 4—Some spark-gaps used for flashover protection a, b, c) Discrete components; (d) printed wiring; (e) integral ('Ring-trap')

## SPARK-GAPS

With the exception of the focus electrode of colour tubes, the same spark-gaps can be used for monochrome and colour tubes. Mechanical considerations limit the gap spacings to about 0·3 to 0·5mm, resulting in a d.c. breakdown voltage of between 2 and 3kV. Spark-gaps for the focus electrode of colour tubes have spacings between 5 and 6mm and a d.c. breakdown voltage of 6 to 8kV. Some of the spark-gaps used at present are shown in Fig. 4. These take the form of discrete units (a, b and c), printed-wiring boards (d), or integral assemblies built into the picture tube ('Ring-trap' base, (e)).

## RESISTORS

Resistors intended for use in flashover protection circuits should be able to withstand peak voltages up to the full e.h.t. value. This also applies to their mountings and to the sockets for the tube base. Carbon composition resistors have been found to be satisfactory in this application. The following values are suggested:

| | |
|---|---|
| cathode | 1·5kΩ |
| grid | 8·2kΩ |
| first anode | 22kΩ |
| focus electrode | |
| monochrome | 22kΩ |
| colour | 100kΩ |

### EFFECTS OF FLASHOVER ON E.H.T. SUPPLY

A simplified equivalent circuit of a line output transformer with third-harmonic tuning is shown in Fig. 5. After a flashover discharge, the picture tube capacitance is completely discharged, and a large number of cycles are needed to restore its potential. During part of this time this capacitance acts as a short circuit, thus placing the leakage inductance $L_2$ across the primary inductance $L_1$. In consequence, the flyback time is halved, and the peak voltage increased by up to 2·5 times. Since most of the energy is diverted to charge the picture tube capacitance, very little is left for the energy recovery. This produces an increase in the peak and average currents, leading to saturation of the output transformer, which results in even higher currents.

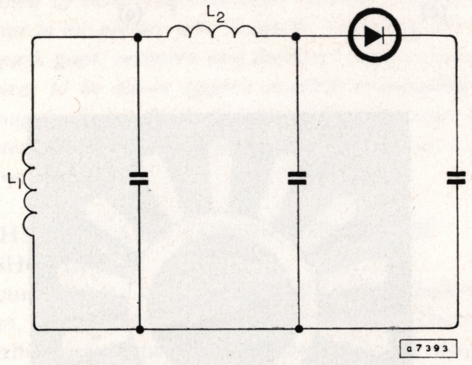

Fig. 5—Equivalent circuit of transformer with third-harmonic tuning

All these effects are observed when the e.h.t. capacitor is discharged by any agency, including a flashover discharge across the e.h.t. rectifier when there is, in addition, an injection of energy into the line timebase circuit.

Protective measures against overload of the e.h.t. supply are always desirable, and are essential when semiconductor devices are driven by the flashover beyond their permissible limits. A simple and effective approach is to arrange an automatic reduction in h.t. potential during overloads. This can be obtained by placing a resistor in series with the h.t. line to the output transformer. Its value should be adjusted to limit the increase in the peak voltage to, say, 20%. The suggested limitation is a compromise between the reduction in the VA-product of the device and the loss in the e.h.t. regulation caused by the presence of the resistor.

Similar results may be obtained with a desaturated line output transformer, provided that a small coupling capacitor is used.

In transistorised equipment, it seems logical that semiconductor diodes will be used as the e.h.t. rectifier. These can be produced to be free from internal flashover.

### RECEIVER TESTING

A triggered spark-gap is convenient for testing receivers in respect of flashover. One terminal of the gap is connected to the e.h.t. contact of the picture tube and the other to a flying lead. The receiver is operated at nominal mains voltage increased by 10%.

The test is started by connecting the flying lead to the focus pin of the picture tube and operating the spark-gap at a rate of about one breakdown in three seconds. After about a hundred discharges, the lead is transferred to the first anode, then to the grid, and so on.

At each stage, observations are made of the discharge on the tube socket, and of the receiver wiring and the general behaviour of the receiver. Every effort is made to trace the path taken by the flashover currents, occasionally removing any unintended spark-gaps within the chassis. When a flashover inside the tube is suspected, the relevant pin is isolated from the circuit by means of series resistors.

Tests on the line timebase are made with a special synchronising unit to operate the triggered spark-gap. This arrangement enables the flashover to be produced at any desired part of the line timebase cycle, and enables observations to be made of the behaviour of the circuit before the discharge and for any length of time afterwards.

---

# C.R.T. Grid Drive Circuit using D.C. Restoration of the Unblanking Signal

G. W. Broekema
Philips Cathode Ray Tube Development Laboratory, Eindhoven

*The circuit described uses d.c. restoration to pass the d.c. component of the unblanking signal to the control grid of the oscilloscope tube, thus eliminating the need for an h.t. bias source. Used in conjunction with a new range of inexpensive oscilloscope tubes this circuit facilitates the construction of low-cost oscilloscopes. The d.c. restoration circuit, several versions of which are described, offers the following benefits: the design is simple; there is no extra drain from the h.t. supply and no additional h.t. bias source; only inexpensive high-voltage capacitors are needed; the circuit is relatively insusceptible to hum; the brightness control is at low d.c. potential. Adaptations with the brightness control at h.t. potential are also shown.*

### INTRODUCTION

A major difficulty in the design of unblanking circuits is the d.c. coupling of the unblanking signal to the control grid of the c.r.t. because this is at very high negative potential. Even at very low sweep rates, the unblanking signal must be passed undistorted to the c.r.t. control grid. If the top of the unblanking pulse is not flat, uneven illumination of the trace will be caused.

Conventional circuits use an h.t. bias source to overcome the high potential difference between the unblanking pulse output stage and the c.r.t. control grid, and either they are complex in design or they constitute an extra load on the c.r.t. supply.

To avoid the drawbacks of h.t. biasing, cathode ray tubes using deflection blanking were introduced a few years ago. Rather than being suppressed as in the case of c.r.t. grid drive, the electron beam is intercepted by deflecting its course. Beam deflection is achieved by applying a potential difference to the deflection blanking plates which are built into the electron gun. The deflection blanking plates are intended to be driven at (or near) earth potential, and can therefore be connected directly to the pulse output stage.

However, the unblanking system must be extremely accurately mounted to avoid spot shift caused by the unblanking pulse. Another drawback is that cathode current continues to flow during the blanking periods. The required cathode current may be very high at high writing speeds when, for example, displaying single-shot events of short duration. The electron gun can be so designed that the cathode is able to carry these high current levels without damage; such a design results, however, in an increased spot size, which affects the image resolution. Nevertheless, the allowable continuous cathode current is lower than the peak value permitted for cathode ray tubes where unblanking is achieved by grid drive. The cathode of the c.r.t. can sustain very high current pulses as a high cathode current density is allowed during a brief instant. Operation at high peak current with moderate average current level, as is attainable with the grid-driven c.r.t., results in high image brilliance together with optimum resolution.

The present article describes a circuit in which the unblanking signal is chopped and restored to negative h.t. level for c.r.t. grid drive, thus avoiding the use of an h.t. bias source. Brightness control at a low d.c. level occurs by adjusting the amplitude of the chopping pulses. This simple circuit is advantageously used in conjunction with two new groups of inexpensive oscilloscope tubes described below.

*D7–190GH, D10–160GH, and D13–480GH*

These are three types of monoaccelerator tubes based on the same gun and intended for use in oscilloscopes and monitoring devices with a bandwidth of up to 10 MHz. As no post-acceleration field is used, the tubes exhibit high image resolution (small spot size), and good geometry performance. Other features are:

1) short length, hence minimum space requirements;
2) high control-grid sensitivity, hence low grid drive requirements;
3) high reliability derived from simple, rugged construction;
4) very high electron gun efficiency, which implies that the screen current is a large percentage of the cathode current.

*D10–170GH, D14–120GH, and D14–121GH*

These offer the advantages of mesh techniques:

1) high deflection sensitivity, making the tubes suitable for transistorised oscilloscopes of 20 to 50MHz bandwidth;
2) modest overall length, which is essential for portable equipment;
3) negligible deflection defocusing;
4) high brightness.

### D.C. RESTORING CIRCUIT

The input terminals A and B in Fig. 1 have a low potential with respect to earth, while the c.r.t. grid carries a high negative potential. Terminal A is connected direct to the unblanking pulse output stage, so the high-frequency

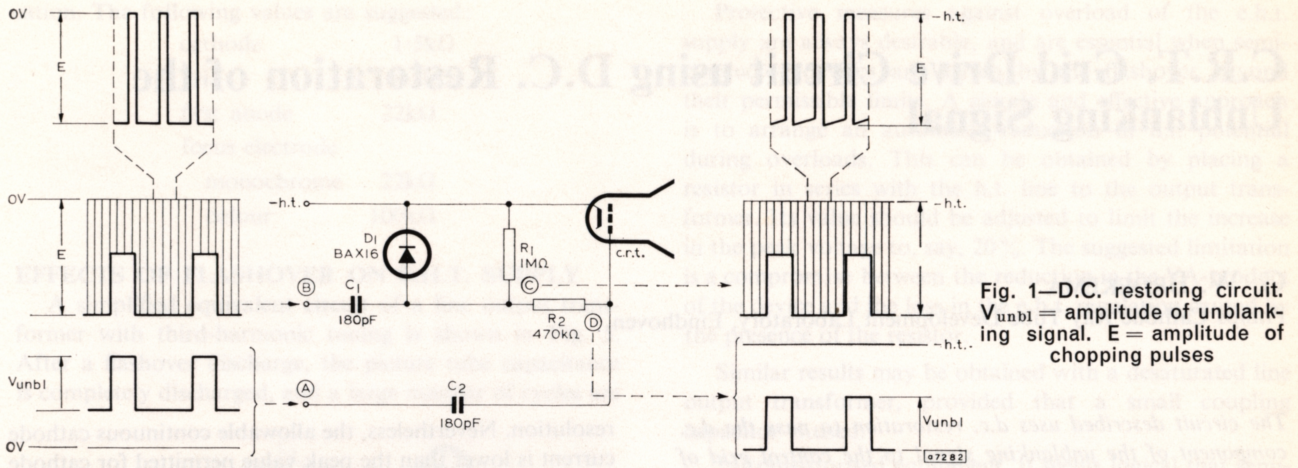

Fig. 1—D.C. restoring circuit. $V_{unbl}$ = amplitude of unblanking signal. E = amplitude of chopping pulses

components of the unblanking signal reach the grid of the c.r.t. via coupling capacitor $C_2$. To supply also the d.c. and low-frequency components to the c.r.t. grid, the input signal is passed via a 200kHz chopper (not shown) and presented via terminal B to network $C_1$, $D_1$, $R_1$. When comparing the chopped waveforms at points B and C, it is seen that the zero level in the waveform at point B is restored to h.t. level.

The performance of the d.c. restoring circuit is more clearly illustrated by the upper waveforms given in Fig. 1. These show the chopped signals at B and C on an extended time scale with the chopper output idealised to a true rectangular waveform. The input signal at terminal B is assumed to be chopped to zero level. The positive chopping pulses cause the restoring diode $D_1$ to conduct. Capacitor $C_1$, which has lost some of its charge via $R_1$ during the previous non-conducting period of $D_1$, is rapidly charged again to h.t. level via the low chopper output resistance (charge time-constant about 0·2μs). Neglecting the forward voltage of the restoring diode, no voltage drop occurs across parallel resistor $R_1$, hence the peaks of the chopping pulses are restored to -h.t. level. Diode $D_1$ is made non-conductive by the trailing edge of the chopping pulses, and the capacitor discharges via $R_1$, so that the potential at its right-hand plate rises slightly towards -h.t. level. The discharge of the capacitor is, however, insignificant because the time-constant $C_1R_1$ (180μs) is much larger than the repetition time (5μs) of the chopping pulses. The capacitor discharge is illustrated by the slightly slanting lines in the upper wave shape at point C. As the restoring diode is reverse-biased in between the chopping pulses, the amplitude E of the chopped signal will appear across parallel resistor $R_1$.

To minimise the loss in d.c. voltage due to chopping and restoring, the chopping pulses must be as short as possible and the time-constant $R_1C_1$ of the restoring circuit must be large compared with the repetition time of the chopping pulses. In view of the high chopping frequency (200kHz), a value of 180pF is adequate for high-voltage capacitor $C_1$. Also, the restoring diode must have minimum leakage (leakage resistance high with respect to $R_1$) and must exhibit fast recovery properties. Silicon oxide passivated diode BAX16, used in the circuit, has a recovery time below 120ns and a residual charge less than 0·7nC.

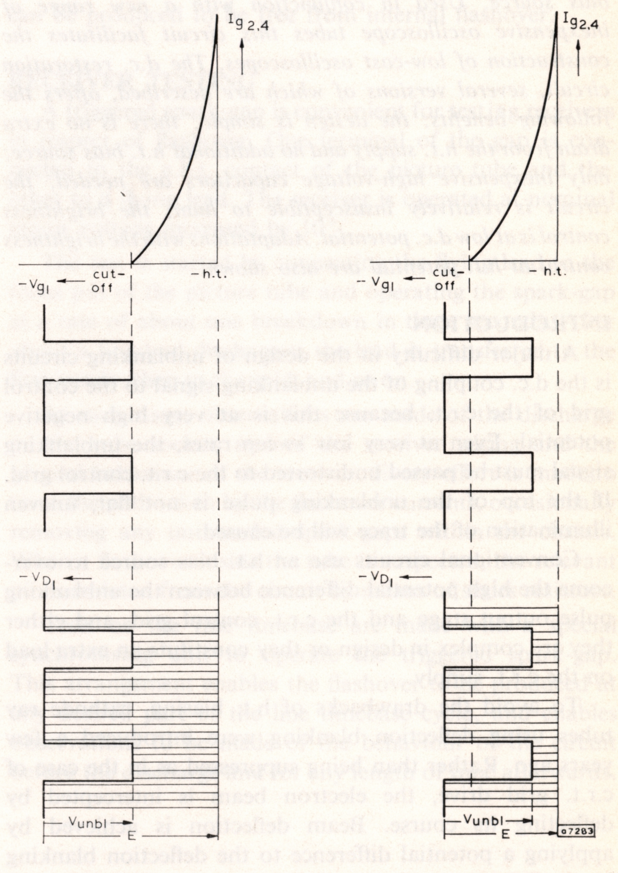

Fig. 2—Principle of brightness control. $V_{unbl}$ = amplitude of unblanking signal. E = amplitude of chopping pulses

The purpose of network $R_2C_2$ is to keep the chopping pulses away from the c.r.t. grid. This network acts as a low-pass filter (integrating action) since terminal A is connected to earth via the low output impedance of the pulse output stage. Neglecting the loss in d.c. voltage due to chopping and restoring, the variations of the d.c. level at points A and C resulting from the unblanking signal may be assumed equal. Thus, the unblanking signal will set up no charge or discharge currents through $R_2$. Hence, the value of $C_2$ is solely determined by the residual ripple allowable at point D. A low value may thus be chosen for $C_2$; this is advantageous from a cost point of view because $C_2$ is a high voltage capacitor. Summarising, we may state that the higher frequencies present in the unblanking signal are passed to the grid of the c.r.t. via $C_2$, the lower frequencies and the d.c. component via the d.c. restoring circuit ($C_1$, $D_1$, $R_1$ and $R_2$).

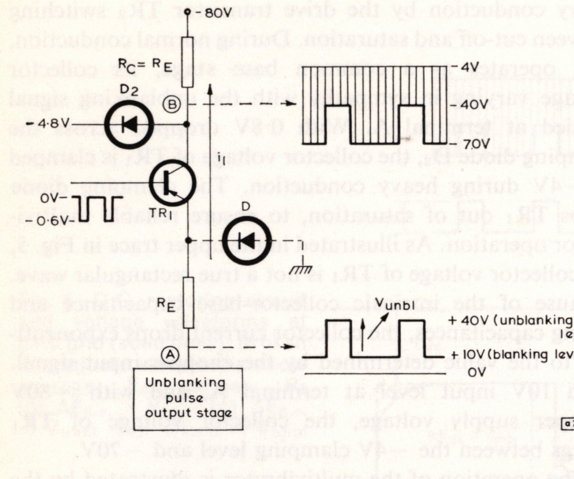

Fig. 3—Chopper circuit

Brightness control at a low d.c. level is accomplished by adjusting the magnitude of the chopping pulses as illustrated in Fig. 2. The necessary control range depends on the cut-off voltage of the c.r.t. and the grid drive needed for maximum brilliance of the trace.

An essential feature of the d.c. restorer is its low susceptibility to hum. As the time-constant of the restoring network is small compared with the period of the mains supply, the d.c. signal will be restored to -h.t. level even with hum superimposed on the negative c.r.t. supply voltage. With the chosen time-constants $R_1C_1$ and $R_2C_2$, the ripple component between the cathode and grid of the c.r.t. is approximately (1/20)×h.t. ripple voltage. Smoothing of the h.t. supply will thus become less critical, in view of allowable intensity modulation.

An analysis of the d.c. restoring and integrating networks is given in Appendix I.

## BRIGHTNESS CONTROL AT LOW D.C. POTENTIAL

The chopper circuit is an astable multivibrator whose operation is explained on page 196. For simplicity, the pass transistor $TR_1$ only is shown in Fig. 3, and a hypothetical diode D is considered as being present in the circuit. Points A and B in the diagram correspond to the input terminals of the d.c. restorer illustrated in Fig. 1. The transistor is periodically brought into heavy conduction by negative pulses (200kHz pulse frequency) applied to its base; heavy transistor conduction during the base drive pulses is achieved because diode D restricts the negative emitter voltage to earth potential. During heavy conduction, the collector voltage is clamped by diode $D_2$ at about -4V for reasons given later.

Because of the pulsatory base drive, the input signal is chopped to the clamping level of the collector voltage; this is also the level of the chopped signal which is restored to the negative c.r.t. supply voltage.

The circuit operates as a common-base stage when the base is not driven negative by the base input pulses (with the base at earth potential). Neglecting the base current, all of the current $i_1$ supplied to the emitter by the unblanking pulse output stage will emerge at the collector. The gain of the grounded base stage is unity as collector resistance $R_C$ and emitter resistance $R_E$ are equal. Denoting the chopper input signal at terminal A by $V_A$ and the chopper output at terminal B by $V_B$, the following equation may be given.

$$V_B = -80V + i_1R_C = -80V + i_1R_E = -80V + V_A \quad \ldots(1).$$

This expression is a good approximation to the actual circuit conditions as the emitter-base voltage drop is small compared with the input signal. Evidently, the chopper input signal will appear at the collector but shifted by the amount of the collector supply voltage (−80V). Stated differently, when the base current and the emitter-base voltage can be assumed to be zero, the voltage drop across $R_C$ is equal to the voltage drop across $R_E$, and this is in turn equal to the chopper input.

To provide for brightness control at a low d.c. level, an adjustable standing current is injected into the emitter of $TR_1$ (Fig. 4). If the standing current is $I_2$, Eq. 1 will be changed to:

$$V_B = -80V + V_A + I_2R_C. \quad \ldots(2)$$

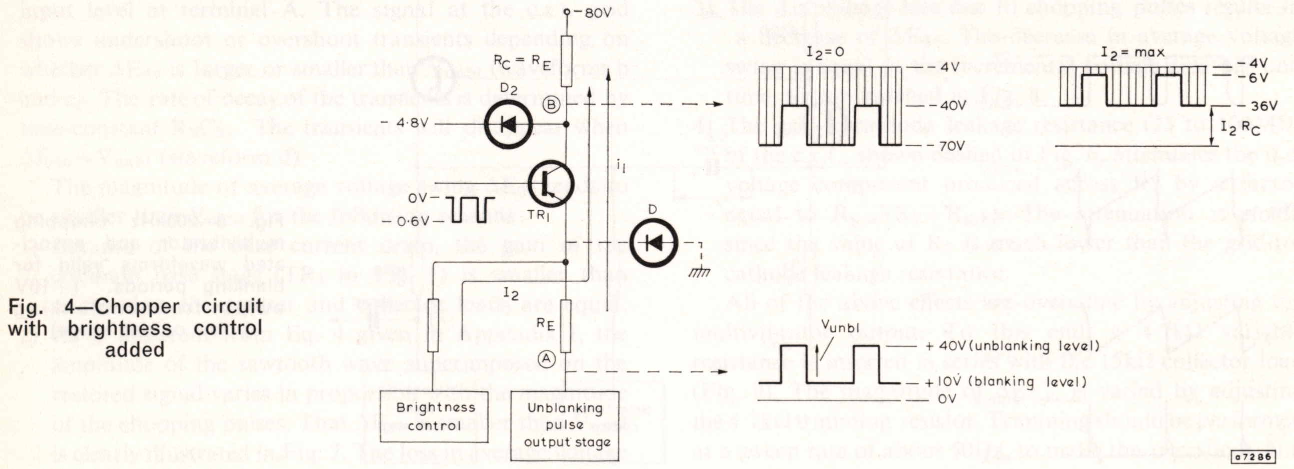

Fig. 4—Chopper circuit with brightness control added

The shift of the collector signal is $I_2R_C$, as illustrated by the collector voltage waveforms in Fig. 4. Increase of $I_2$ will diminish the magnitude of the chopping pulses; this reduces the negative bias on the c.r.t. grid during unblanking and so increases the brightness of the trace. The minimum amplitude of the chopping pulses, allowed in view of correct chopper operation, is about 2V (see the right hand collector voltage waveform in Fig. 4); this gives sufficient image brilliance for any of the quoted types of c.r.t. at maximum setting.

The voltage fluctuations, created by the pulsating base drive, at the emitter of $TR_1$ must not disturb the unchopped signal at terminal A. This means that the output impedance of the unblanking pulse output stage must be low with respect to $R_E$. In the actual circuit the emitter voltage fluctuations are approximately 0·5V. If $R_E$ is 15kΩ and if we assume that the output impedance of the unblanking pulse output stage is 0·5kΩ, the superimposed ripple due to chopping is $0{\cdot}5 \times 0{\cdot}5/15{\cdot}5 = 16\text{mV}$, which is negligible. It is worth noting that ripple superimposed on the negative supply of the chopper will not affect the operation of the circuit provided that the minimum amplitude of the chopping pulses exceeds 2V. The collector current of the pass transistor and thus the amplitude of the chopping pulses is then entirely determined by the emitter current.

## CHOPPING MULTIVIBRATOR

The chopper circuit (Fig. 5) is an astable multivibrator. The pass transistor $TR_1$ is switched between normal and heavy conduction by the drive transistor $TR_2$ switching between cut-off and saturation. During normal conduction, $TR_1$ operates as a common base stage, its collector voltage varying in sympathy with the unblanking signal applied at terminal A. With 0·8V dropped across the clamping diode $D_2$, the collector voltage of $TR_1$ is clamped at −4V during heavy conduction. The clamping diode keeps $TR_1$ out of saturation, to ensure reliable multivibrator operation. As illustrated in the upper trace in Fig. 5, the collector voltage of $TR_1$ is not a true rectangular wave. Because of the intrinsic collector-base capacitance and wiring capacitances, the collector current drops exponentially to the value determined by the chopper input signal. With 10V input level at terminal A, and with −80V chopper supply voltage, the collector voltage of $TR_1$ swings between the −4V clamping level and −70V.

The operation of the multivibrator is illustrated by the waveforms given in Fig. 5. With $TR_2$ cut off ($v_{eb} = +0{\cdot}6\text{V}$), the base of $TR_1$ is at 0V ($TR_1$ operating as common base stage). $C_3$ is charged negatively at a constant rate via $R_3$ towards −80V, pulling the emitter of $TR_2$ negatively. Transistor $TR_2$ starts to draw current as soon as its base-emitter junction becomes forward biased. The loop gain of $TR_1$, $TR_2$ increases from a value below unity as the base current of $TR_2$ rises. When the loop gain exceeds unity, $TR_2$ switches into saturation. Its collector voltage drops to −0·6V bringing $TR_1$ into heavy conduction; clamping diode $D_2$ keeps $TR_1$ out of saturation ($-V_{CE(min)} = 4\text{V}$). Capacitor $C_3$ rapidly discharges via the emitter of $TR_2$, despite the charge current through $R_3$. When the capacitor discharge current has sufficiently decreased, the collector current of $TR_2$ starts to drop and the loop gain can thus increase beyond unity. $TR_2$ is then cut off ($v_{eb}$ rising to $+0{\cdot}6\text{V}$), and $TR_1$ is switched to normal conduction. Capacitor $C_3$ starts to charge again at a constant rate towards −80V, to repeat the cycle. The multivibrator repetition frequency depends on time-constant $R_3C_3$ and is about 200kHz in this circuit.

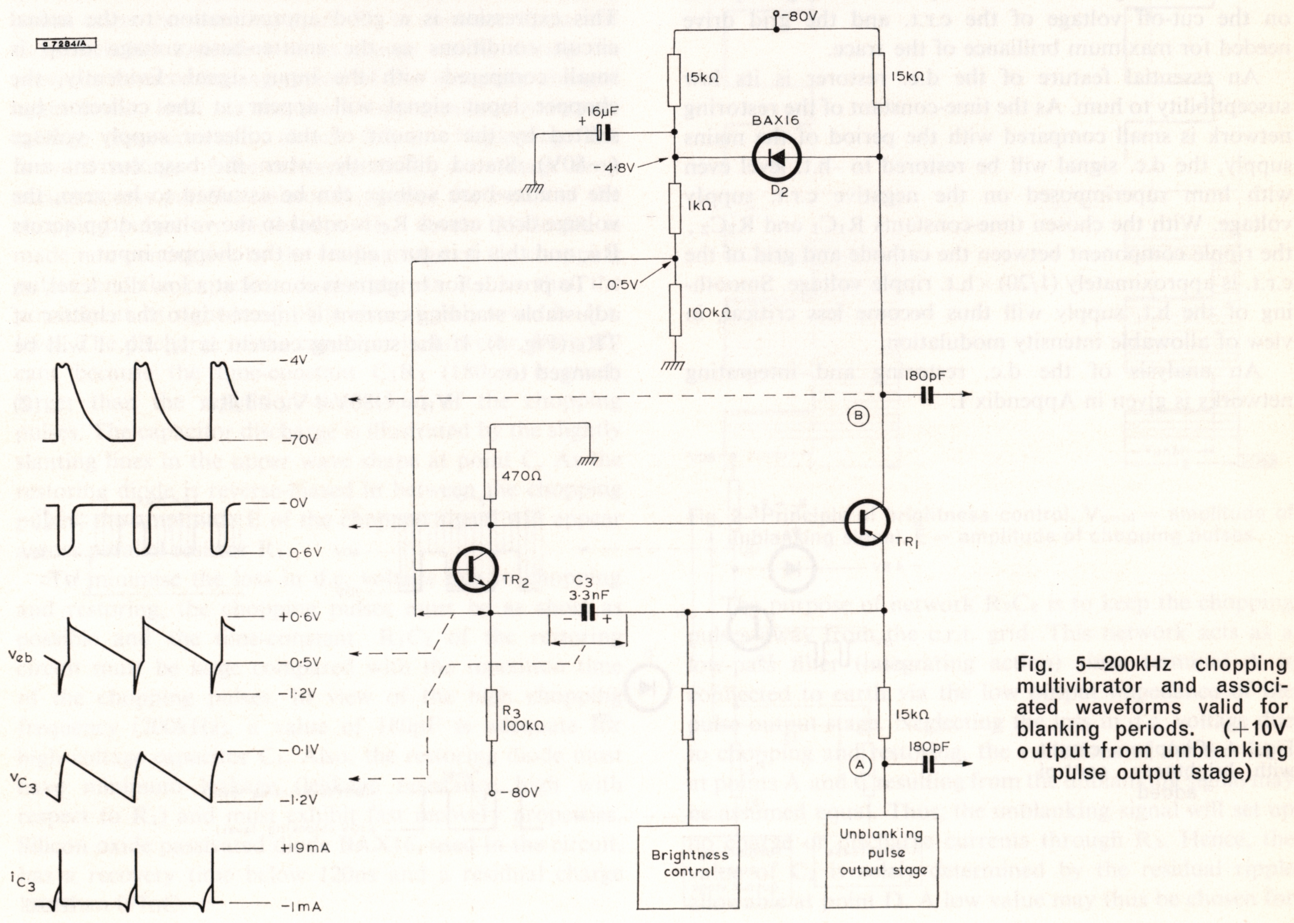

Fig. 5—200kHz chopping multivibrator and associated waveforms valid for blanking periods. (+10V output from unblanking pulse output stage)

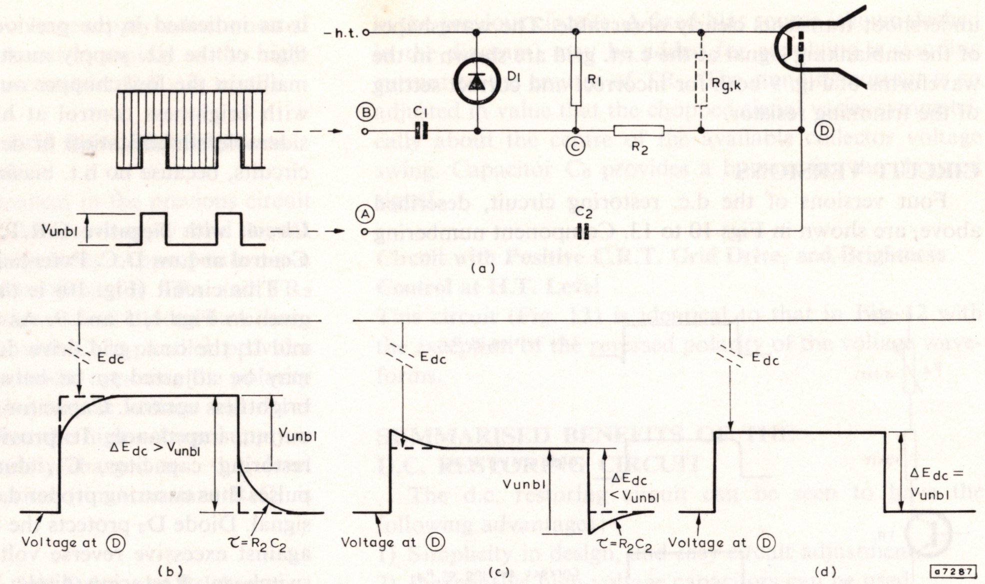

Fig. 6—D.C. restoring circuit and voltage waveforms at c.r.t. grid (solid lines). Broken line square waveforms show average $E_{d.c.}$ across $R_1$ (b) $\Delta E_{d.c.} > V_{unbl}$ (c) $\Delta E_{d.c.} < V_{unbl}$ (d) $\Delta E_{d.c.} = V_{unbl}$

## ADJUSTMENT OF THE MULTIVIBRATOR OUTPUT

The top of the unblanking pulse must be sufficiently flat to maintain even brightness of the c.r.t. trace. One of the merits of the d.c. restorer is that this can be easily achieved by adjusting the output of the chopping multivibrator.

The circuit diagram of the d.c. restorer is redrawn in Fig. 6, together with the waveforms of the unblanking signal at the c.r.t. grid (point D). In steady-state condition, no charge or discharge current flows through $R_2$, and the d.c. voltage at D is equal to the average voltage $E_{dc}$ across $R_1$. Thus, if the swing in average voltage across $R_1$ due to the unblanking signal ($\Delta E_{dc}$) is not equal to the magnitude of the unblanking pulse ($V_{unbl}$), then $C_2$ will be slightly charged and discharged during each change in d.c. input level at terminal A. The signal at the c.r.t. grid shows undershoot or overshoot transients depending on whether $\Delta E_{dc}$ is larger or smaller than $V_{unbl}$ (waveforms b and c). The rate of decay of the transients is determined by time-constant $R_2C_2$. The transients will disappear when $\Delta E_{dc} = V_{unbl}$ (waveform d).

The magnitude of average voltage swing $\Delta E_{dc}$ tends to be smaller than $V_{unbl}$ for the following reasons:

1) Because of the base current drain, the gain of the common base stage ($TR_1$ in Fig. 5) is smaller than unity when the emitter and collector loads are equal.
2) As is apparent from Eq. 4 given in Appendix I, the amplitude of the sawtooth wave superimposed on the restored signal varies in proportion with the magnitude of the chopping pulses. That $\Delta E_{dc}$ is smaller than $V_{unbl}$ is clearly illustrated in Fig. 7. The loss in average voltage swing due to this effect is of minor importance since the sawtooth ripple is small (a few per cent).
3) The d.c. voltage loss due to chopping pulses results in a decrease of $\Delta E_{dc}$. The decrease in average voltage swing is equal to the incremental voltage area per unit time, shown hatched in Fig. 8.
4) The grid-to-cathode leakage resistance (25 to 100MΩ) of the c.r.t., shown dashed in Fig. 6, attenuates the d.c. voltage component produced across $R_1$ by a factor equal to $R_{g,k}/(R_2+R_{g,k})$. The attenuation is small, since the value of $R_2$ is much lower than the grid-to-cathode leakage resistance.

All of the above effects are overcome by adjusting the multivibrator output. To this end, a 4·7kΩ variable resistance is inserted in series with the 15kΩ collector load (Fig. 9). The magnitude of $\Delta E_{d.c.}$ is varied by adjusting the 4·7kΩ trimming resistor. Trimming should be performed at a sweep rate of about 50Hz, to make the overshoot and

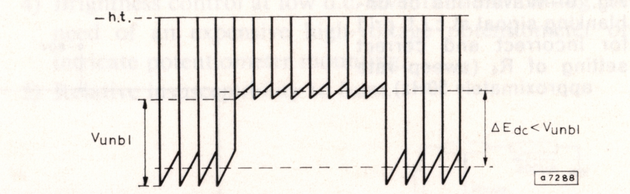

Fig. 7—Loss in average voltage swing due to dependence of sawtooth amplitude on magnitude of chopping pulses ($\Delta E_{d.c.} < V_{unbl}$)

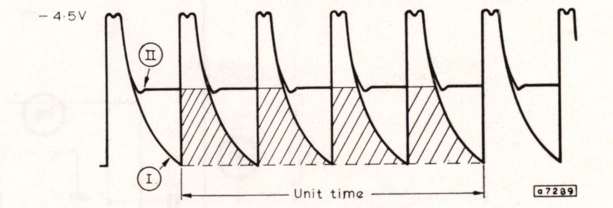

Fig. 8—Oscillogram waveforms of chopping pulses during blanking (trace I) and unblanking (trace II). The hatched area per unit time represents the loss in average voltage swing

undershoot transients clearly observable. The waveshapes of the unblanking signal at the c.r.t. grid are shown in the waveforms of Fig. 9 both for incorrect and correct setting of the trimming resistor.

## CIRCUIT VERSIONS

Four versions of the d.c. restoring circuit, described above, are shown in Figs 10 to 13. Component numbering is as indicated in the previous diagrams. The smoothing filter of the h.t. supply must have a *capacitive* output to maintain the low chopper output impedance. The circuits with brightness control at high potential still offer considerable simplification in design compared with existing circuits, because no h.t. biasing source is employed.

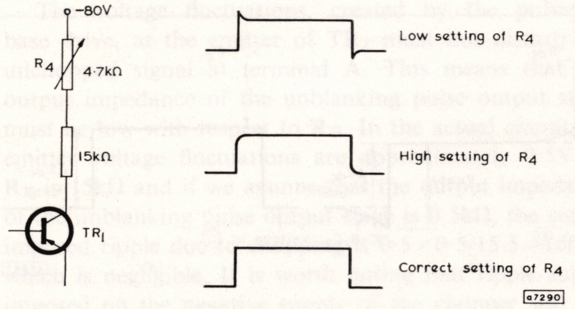

Fig. 9—Waveforms of unblanking signal at c.r.t. grid for incorrect and correct setting of $R_4$ (sweep rate approximately 50Hz)

### Circuit with Negative C.R.T. Grid Drive, and Brightness Control at Low D.C. Potential

This circuit (Fig. 10) is the composite circuit of those given in Figs 1, 5 and 9. As apparent from waveforms I and II, the c.r.t. grid drive during the unblanking periods may be adjusted to be between −36 and −2V by the brightness control. Capacitor $C_4$ establishes a low chopper output impedance. It provides rapid charging of the restoring capacitor, $C_1$, during the positive chopping pulses thus ensuring proper d.c. restoration of the chopped signal. Diode $D_3$ protects the base-emitter junction of $TR_1$ against excessive reverse voltages that may occur during switch-on. Restoring diode $D_1$ will suffer no excessive reverse voltage when the high-voltage supply is disconnected because $C_1$ then discharges almost as rapidly as the high-voltage filter capacitors (time-constant $C_1R_1$ is small).

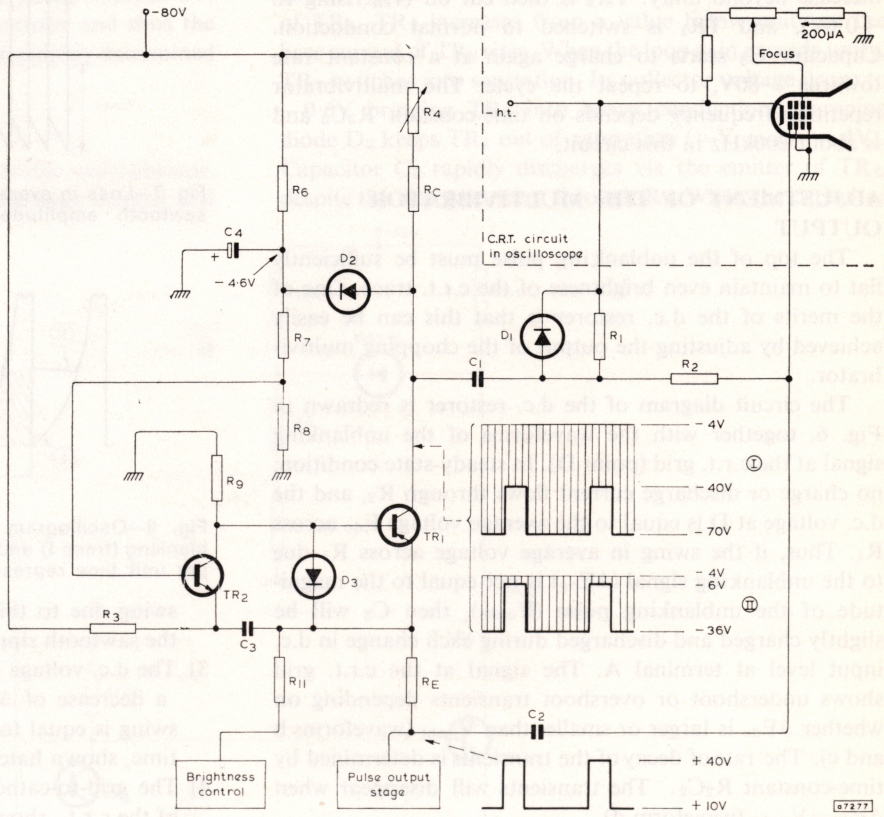

Fig. 10—D.C. restoring circuit with negative c.r.t. grid drive and brightness control at low d.c. potential

|  |  |  |  |
|---|---|---|---|
| $R_1$ | 1MΩ | ±5% | ¼W |
| $R_2$ | 170kΩ | ±5% | ¼W |
| $R_3$ | 100kΩ | ±5% | ¼W |
| $R_4$ | 4·7kΩ | ±20% | potentiometer linear |
| $R_6$ | 15kΩ | ±5% | ¼W |
| $R_7$ | 820Ω | ±5% | ⅛W Style CR25 |
| $R_8$ | 100Ω | ±5% | ⅛W Style CR25 |
| $R_9$ | 470Ω | ±5% | ⅛W Style CR25 |
| $R_{11}$ | 15kΩ | ±5% | ¼W |
| $R_E$ | 15kΩ | ±5% | ¼W |
| $R_C$ | 15kΩ | ±5% | ¼W |
| $C_1$, $C_2$ | 180pF | 2000V ceramic | |
| $C_3$ | 3·3nF | ±10% 160V polyester C296AA/A3K3 | |
| $C_4$ | 16µF | −10%+50% 10V electrolytic C426AR/D16 | |
| $D_1$, $D_2$ | BAX16 | | |
| $D_3$ | AA119 | | |
| $TR_1$ | AF118 | | |
| $TR_2$ | BF194 | | |

### Circuit with Positive C.R.T. Grid Drive, and Brightness Control at Low D.C. Potential

This circuit (Fig. 11) is identical to the previous circuit with the exception of the chopper supply and signal voltages which are reversed in polarity. Appropriate n-p-n and p-n-p transistors are substituted for $TR_1$ and $TR_2$ respectively, and the connections of all diodes have been reversed. Stabilising diode $D_4$, with $C_5$ in parallel, provides a positive bias for the c.r.t. cathode, opposing the polarity of the grid signal. No excessive reverse voltage will occur across restoring diode $D_1$ when the high-voltage supply is connected, because $C_1$ is rapidly charged to −h.t. level during the first rectifying period (time-constant $R_1C_1$ is small).

### Circuit with Negative C.R.T. Grid Drive, and Brightness Control at H.T. Level

Brightness control in this circuit (Fig. 12) is achieved by adjusting resistor $R_{12}$. The chopper supply voltage has been decreased to 60V because the chopping pulses are not varied in magnitude by shifting the chopped signal as in the previous circuits. A fixed bias source (shown dashed in the diagram) may be added for supplying a standing current to the emitter of $TR_1$. The standing current is so adjusted in value that the chopped signal varies symmetrically about the centre of the available collector voltage swing. Capacitor $C_6$ provides a by-pass for the chopped signal.

### Circuit with Positive C.R.T. Grid Drive, and Brightness Control at H.T. Level

This circuit (Fig. 13) is identical to that in Fig. 12 with the exception of the reversed polarity of the voltage waveforms.

## SUMMARISED BENEFITS OF THE D.C. RESTORING CIRCUIT

The d.c. restoring circuit can be seen to have the following advantages:

1) Simplicity in design, and easy circuit adjustment.
2) Inexpensive high-voltage capacitors can be used.
3) No extra current drain from the h.t. supply source.
4) Brightness control at low d.c. level thus eliminating the need of an expensive high-voltage potentiometer or intricate potentiometer mounting.
5) Relative insusceptibility to hum.

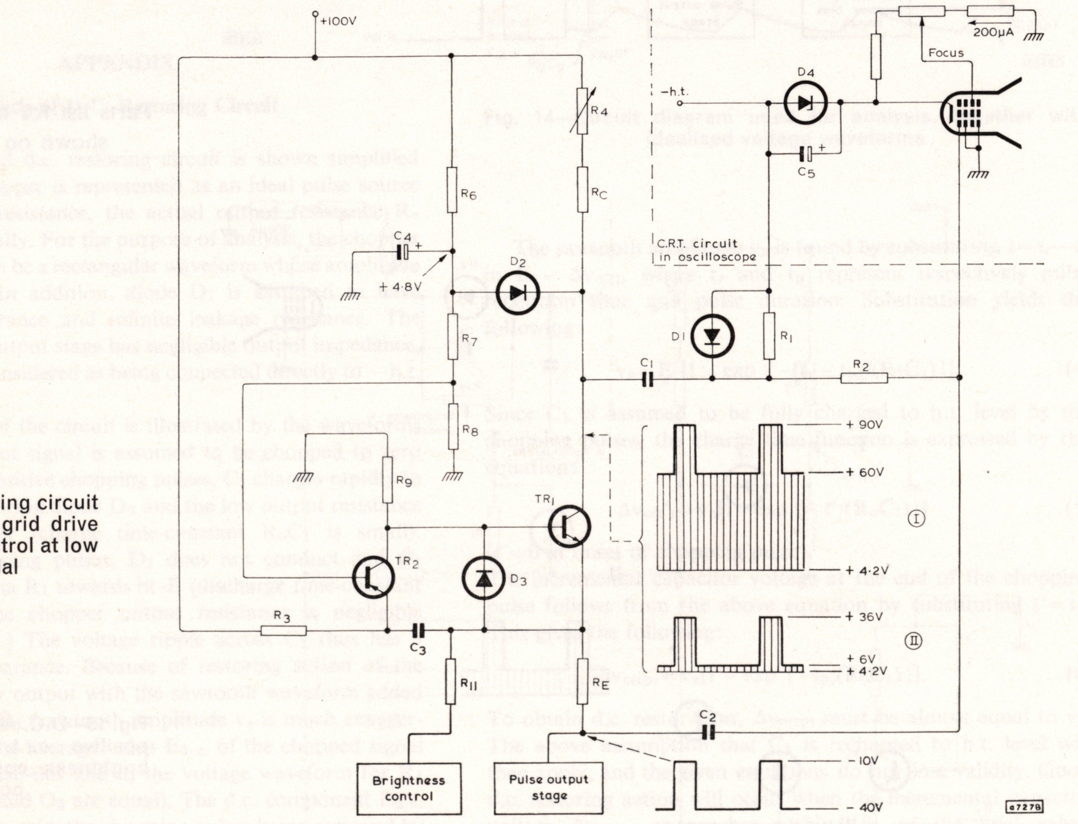

Fig. 11—D.C. restoring circuit with positive c.r.t. grid drive and brightness control at low d.c. potential

PARTS LIST (Fig. 11)

Components not stated below are identical to those quoted for Fig. 10.

|  |  |  |  |
|---|---|---|---|
| $R_3$ | 120kΩ | ±5% | ¼W |
| $R_6$ | 22kΩ | ±5% | ½W |
| $R_7$ | 1kΩ | ±5% | ⅛W Style CR25 |
| $R_c$ | 15kΩ | ±5% | 1W |
| $C_5$ | 6·4µF | 150V | electrolytic |
| $D_4$ | BZY95—C75 | | |
| $TR_1$ | BSX21 | | |
| $TR_2$ | BC187 | | |

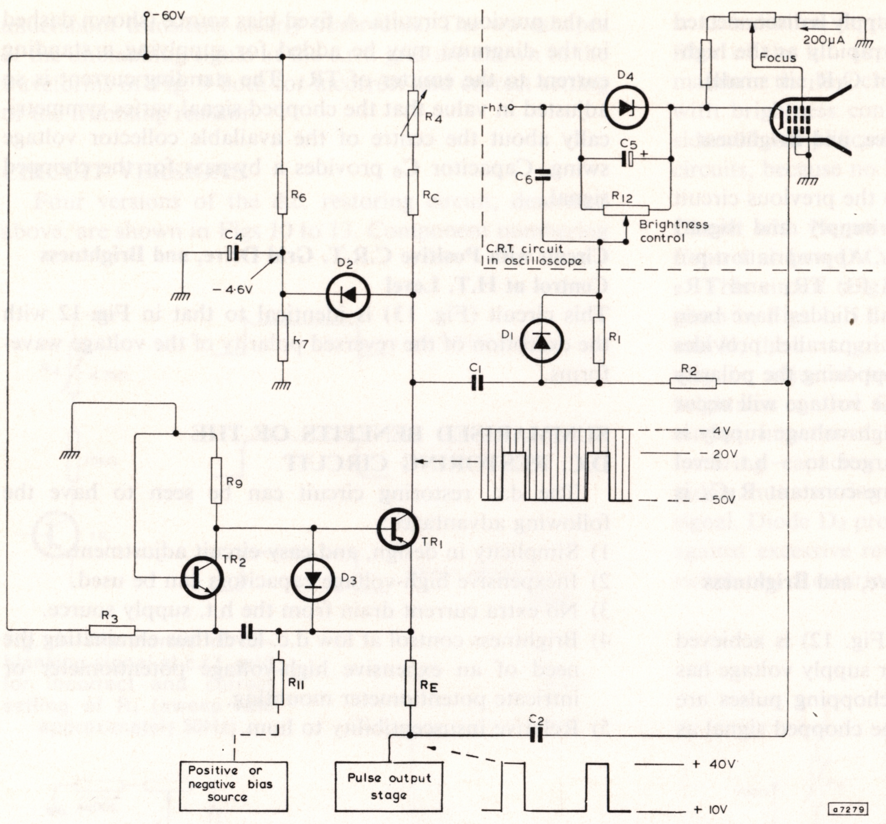
-60V
200µA
Focus
D4
h.t.o
R4
C5
C6
R12
Brightness control
R6
RC
C4
-4·6V
D2
C.R.T. circuit in oscilloscope
R7
D1
R1
C1
R2
-4V
-20V
-50V
R9
TR1
TR2
D3
R3
C3
R11
RE
C2
Positive or negative bias source
Pulse output stage
+40V
+10V
67279

Fig. 12—D.C. restoring circuit with negative c.r.t. grid drive and brightness control at high d.c. potential

Parts list for figs. 12 and 13 are shown on page 201.

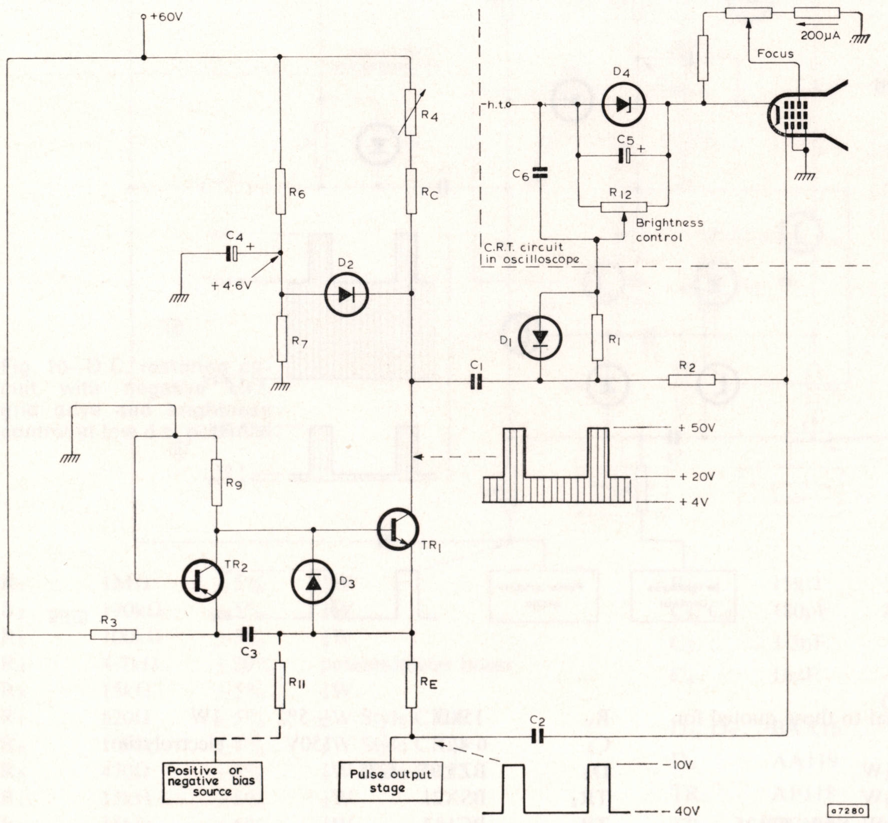
+60V
200µA
Focus
D4
h.t.o
R4
C5
C6
R12
Brightness control
R6
RC
C4
+4·6V
D2
C.R.T. circuit in oscilloscope
R7
D1
R1
C1
R2
+50V
+20V
+4V
R9
TR1
TR2
D3
R3
C3
R11
RE
C2
Positive or negative bias source
Pulse output stage
-10V
-40V
67280

Fig. 13—D.C. restoring circuit with positive c.r.t. grid drive and brightness control at high d.c. potential

PARTS LIST (Fig. 12)
Components not stated below are identical to those quoted for Fig. 10.

| | | | |
|---|---|---|---|
| $R_6$ | 12kΩ | ±5% | ½W |
| $R_7$ | 1kΩ | ±5% | ½W Style CR25 |
| $R_{12}$ | 470kΩ | ±20% | potentiometer linear |
| $C_5$ | 1µF | | 40V electrolytic C426AS/G1 |
| $C_6$ | 22nF | | 160V polyester C296AA/A22K |
| $D_4$ | BZY95—C30 | | |

PARTS LIST (Fig. 13)
Components not stated below are identical to those quoted for Fig. 10.

| | | | |
|---|---|---|---|
| $R_6$ | 12kΩ | ±5% | ½W |
| $R_7$ | 1kΩ | ±5% | ½W Style CR25 |
| $R_{12}$ | 470kΩ | ±20% | potentiometer linear |
| $C_5$ | 6·4µF | | 150V electrolytic |
| $C_6$ | 22nF | | 160V polyester C296AA/A22K |
| $D_4$ | BZY95—C75 | | |
| $TR_1$ | BSX21 | | |
| $TR_2$ | BC187 | | |

## APPENDIX

### Analysis of D.C. Restoring Circuit

The chopper and d.c. restoring circuit is shown simplified in Fig. 14. The chopper is represented as an ideal pulse source with zero output resistance, the actual output resistance $R_o$ being added externally. For the purpose of analysis, the chopper output is assumed to be a rectangular waveform whose amplitude is denoted by E. In addition, diode $D_1$ is assumed to have zero forward resistance and infinite leakage resistance. The unblanking pulse output stage has negligible output impedance, hence $C_2$ may be considered as being connected directly to −h.t. potential.

The operation of the circuit is illustrated by the waveforms in Fig. 14; the input signal is assumed to be chopped to zero level. During the positive chopping pulses, $C_1$ charges rapidly to −h.t. level via restoring diode $D_1$ and the low output resistance $R_o$ of the chopper (charge time-constant $R_oC_1$ is small). Between the chopping pulses, $D_1$ does not conduct and $C_1$ discharges slowly via $R_1$ towards ht–E (discharge time-constant $R_1C_1$ is large. The chopper output resistance is negligible compared with $R_1$.) The voltage ripple across $C_1$ thus has a sawtooth-like appearance. Because of restoring action of the circuit, the chopper output with the sawtooth waveform added will appear across $R_1$ (sawtooth amplitude $v_z$ is much exaggerated in Fig. 14). The average value $E_{d.c.}$ of the chopped signal is shown by the dash-dot line in the voltage waveform for $R_1$ (hatched areas $O_1$ and $O_2$ are equal). The d.c. component $E_{d.c.}$ is passed to the c.r.t. grid, the chopping pulses being removed by the integrating network $R_2C_2$.

For proper d.c. restoring action, $C_1$ must be fully charged to h.t. level by the chopping pulses. The discharge function for $C_1$ may then be expressed as:

$$\Delta v_{c(t)} = E \exp\{-t/(R_1 C_1)\} \qquad \ldots(3)$$

(t=0 at termination of chopping pulse).

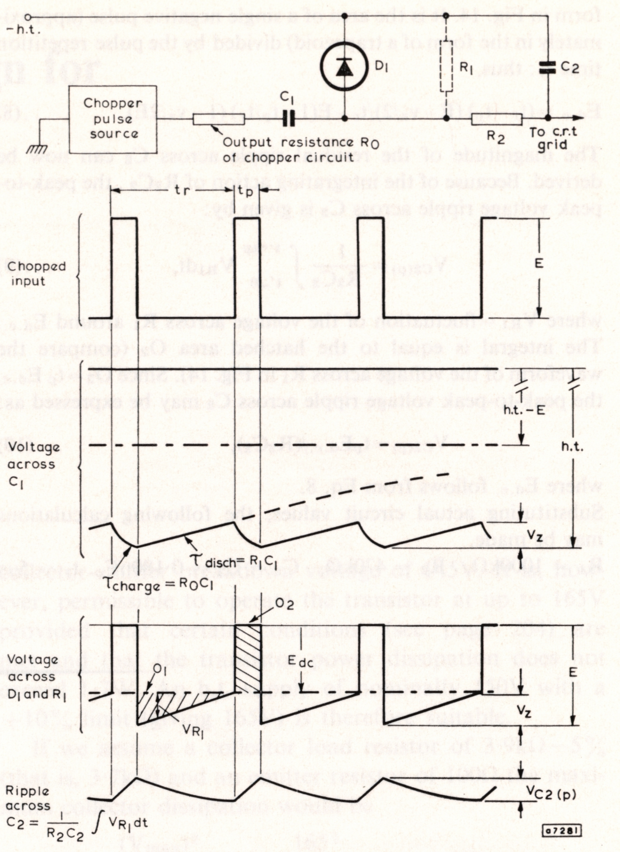
-h.t.
Chopper pulse source
C1
D1
R1
C2
R2
To c.r.t grid
Output resistance RO of chopper circuit
tr
tp
Chopped input
E
h.t.-E
h.t.
Voltage across C1
vz
tdisch=R1C1
tcharge=ROC1
O2
O1
Edc
E
Voltage across D1 and R1
VR1
vz
Ripple across C2 = 1/(R2C2) ∫ VR1 dt
VC2 (p)
67281

Fig. 14—Circuit diagram used for analysis, together with idealised voltage waveforms

The sawtooth amplitude $v_z$ is found by substituting $t=t_r-t_p$ in $E-\Delta v_{c(t)}$, where $t_r$ and $t_p$ represent respectively pulse repetition time and pulse duration. Substitution yields the following:

$$v_z = E\,[1-\exp\{-(t_r-t_p)/(R_1C_1)\}]. \qquad \ldots(4)$$

Since $C_1$ is assumed to be fully charged to h.t. level by the chopping pulses, the charge time function is expressed by the equation:

$$\Delta v_{c(t')} = v_z[1-\exp\{-t'/(R_oC_1)\}] \qquad \ldots(5)$$

($t'=0$ at onset of chopping pulse).
The incremental capacitor voltage at the end of the chopping pulse follows from the above equation by substituting $t'=t_p$. This gives the following:

$$\Delta v_{c(tp)} = v_z[1-\exp\{-t_p/(R_oC_1)\}]. \qquad \ldots(6)$$

To obtain d.c. restoration, $\Delta v_{c(tp)}$ must be almost equal to $v_z$. The above assumption that $C_1$ is recharged to h.t. level will then apply, and the given equations do not lose validity. Good d.c. restoring action will occur when the incremental capactor voltage $\Delta v_{c(tp)}$ approaches within 1% of the final value. Substituting in Eq. 6 the value $\Delta v_{c(tp)} \geqslant 0{\cdot}99 v_z$ the maximum allowable value $R_{o(max)}$ of the chopper circuit can be derived from Eq. 7;

$$0{\cdot}01 = \exp\{-t_p/(R_{o(max)}\,C_1)\}. \qquad \ldots(7)$$

The d.c. component $E_{d.c.}$ of the chopped and restored signal across $R_1$ is readily found from the appropriate voltage waveform in Fig. 14. It is the area of a single negative pulse (approximately in the form of a trapezoid) divided by the pulse repetition time $t_r$: thus,

$$E_{d.c.}=(t_r-t_p)(E-v_z/2)/t_r-E(1-t_p/t_r)(1-v_z/2E). \qquad \ldots(8)$$

The magnitude of the residual ripple across $C_2$ can now be derived. Because of the integrating action of $R_2C_2$, the peak-to-peak voltage ripple across $C_2$ is given by:

$$V_{C2(p)}=\frac{1}{R_2C_2}\int_{t'=0}^{t'=tp} V_{R1}dt, \qquad \ldots(9)$$

where $V_{R1}$ = fluctuation of the voltage across $R_1$ around $E_{d.c.}$. The integral is equal to the hatched area $O_2$ (compare the waveform of the voltage across $R_1$ in Fig. 14). Since $O_2=t_p E_{d.c.}$ the peak-to-peak voltage ripple across $C_2$ may be expressed as:

$$V_{C2(p)}=t_pE_{d.c.}/(R_2C_2), \qquad \ldots(10)$$

where $E_{d.c.}$ follows from Eq. 8.

Substituting actual circuit values, the following calculations may be made.

$R_1 = 1000\text{k}\Omega$, $R_2 = 470\text{k}\Omega$, $C_1 = C_2 = 0{\cdot}180\text{nF}$, $t_r = 5\mu\text{s}$ (chopping frequency 200kHz), $t_p \simeq 1\mu\text{s}$. From Eq. 4, the sawtooth amplitude $v_z$ is found:

$$\begin{aligned}v_z&=E[1-\exp\{-(5-1)/(1000\times0{\cdot}180)\}]\\&=E[1-\exp(-0{\cdot}022)]=E(1-0{\cdot}978)\\&=0{\cdot}022E.\end{aligned}$$

From Eq. 7, $t_p/(R_{o(max)}C_1)=4{\cdot}61$,

$$R_{o(max)}=t_p/(4{\cdot}61C_1)=1/(4{\cdot}61\times0{\cdot}180)=1{\cdot}2\ \text{k}\Omega.$$

From Eq. 8, since $v_z/E=0{\cdot}022$:

$$\begin{aligned}E_{d.c.}&=E(1-1/5)(1-0{\cdot}011)\\&=0{\cdot}8\times0{\cdot}989E=0{\cdot}791E.\end{aligned}$$

Thus, the loss in d.c. voltage is 20% due to chopping and 1·1% due to the superimposed sawtooth waveform.

The peak-to-peak ripple across $C_2$ is calculated from Eq. 10 thus:

$$V_{C2(p)}=\frac{1}{470\times0{\cdot}180}\times1\times0{\cdot}791E=0{\cdot}0093E.$$

The magnitude of the chopping pulse is thus attenuated by a factor of 107 as a result of the integrating action of filter $R_2C_2$.

---

# Transistor Video Amplifier Design for Monochrome TV Receivers

M. C. Gander
Mullard Central Application Laboratory

*A design procedure for monochrome television video amplifiers is given. A practical circuit is described, employing the BF178, for use in monochrome receivers. This design also incorporates picture tube beam current limiting and flyback blanking.*

## INTRODUCTION

As a further step towards fully 'transistorised' monochrome television receiver designs, the use of high voltage transistors in the video output stages is becoming more attractive. Good long term stability and reliability ensue, together with exceptional linearity. The latter, together with the adoption of a low-level sync separation technique (which avoids the picture smearing associated with a valve sync separator driven from the video output) gives the possibility of a high quality picture with simple h.f. compensation.

Necessary points of attention with all video transistors are that excessive power dissipation must be avoided in the transistor and protection must be provided against the possibility of e.h.t. flashover in the picture tube.

This article gives a design procedure based on the BF178 transistor, to provide video signal in excess of 100V peak-to-peak. The BF178 transistor is capable of providing more than 100V black to white picture tube drive under nominal conditions with adequate bandwidth for the U.K. 625-line system. It can be employed in a hybrid receiver by means of a split collector load resistance network which derives +150V from the main h.t. rail.

The circuit described is fully d.c. coupled with constant black level contrast control and has simple but effective means of flyback blanking and beam current limiting for the picture tube.

## CIRCUIT DESIGN OF OUTPUT STAGE

### Collector Load Resistance and Power Dissipation

Although, ideally, the collector load resistor value is determined by bandwidth and gain, in most practical cases the chief determining parameter is the maximum permitted power dissipation in the transistor.

The BF178 data gives a maximum permitted dissipation of 1·7W using a suitable heat dissipator, with a minimum collector-emitter breakdown voltage of 145V. It is, however, permissible to operate the transistor at up to 165V provided that certain conditions (see page 204) are met and that the transistor power dissipation does not exceed 1·7W. An h.t. supply of nominally 150V with a +10% limit (giving 165V) is therefore suitable.

If we assume a collector load resistor of 3·9kΩ−5% (that is, 3·7kΩ) and an emitter resistor of 100Ω the maximum collector dissipation would be

$$\frac{(V_{max})^2}{4R_{L(min)}}=\frac{165^2}{4(3{\cdot}7+0{\cdot}1)10^3}=1{\cdot}8\text{W}.$$

This is higher than the permitted value but if flyback blanking is carried out in the video stage the maximum dissipation will be less than this by at least 15% giving 1·5W.

Fig. 1 shows the operating conditions for the BF178 with a nominal supply voltage of 150V and a 3·9kΩ collector load. Various deductions from the supply voltage are made to find the maximum available drive amplitude as follows:

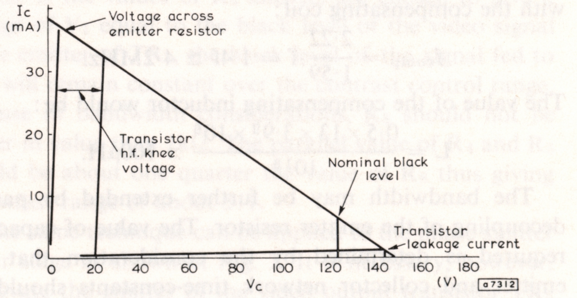

Fig. 1—Operating conditions for BF178 with 3·9kΩ load resistor

1) Typically up to about 5V, caused by transistor leakage current flowing in the collector load.
2) Typically 20V for the h.f. knee voltage of the transistor.
3) Approximately 5V maximum signal excursion across the emitter resistor.

This leaves 120V to accommodate the output signal; about 20V of this should be reserved for the blanking excursion.

For the maximum dissipation of 1·7W, a suitable heat dissipator is necessary. The maximum permitted junction temperature is 200°C. If a maximum ambient cabinet temperature of 55°C is assumed, the total thermal resistance between the junction and ambient should not exceed $\theta_{tot}$, where

$$\theta_{tot} \leqslant \frac{T_j - T_{amb}}{1{\cdot}7}$$
$$\leqslant 85\text{degC/W}.$$

If a side mounting clip (type 56265) is used to affix the transistor to the heat sink

$$\theta_{tot} = \theta_{j\text{-case}} + \theta_{clip+h.s.}.$$

Thus, with $\theta_{j\text{-case}} = 70\text{degC/W}$ (BF178 data),

$$\theta_{clip+h.s.} \leqslant 85 - 70 \leqslant 15\text{degC/W}.$$

As an example, this would require a heat dissipator of approximately 30cm² of blackened aluminium, 1·5mm thick, and mounted vertically.

**Collector Network Bandwidth**

The total collector network capacitance in a well laid out receiver would be typically as follows.

| | | |
|---|---|---|
| Picture tube cathode, plus base, plus lead | = | 7pF |
| Heat dissipator | = | 3pF |
| BF178 output capacitance | = | 3pF |
| Total capacitance, $C_T$ | = | 13pF |

The uncompensated −3dB bandwidth of the network with a 3·9kΩ load resistor is

$$f = \frac{1}{2\pi C_T R_L} \simeq 3\text{MHz}.$$

A shunt compensating coil having the value (Ref. 1)

$$L = nC_T R_L{}^2$$

where n = 0·5, can be employed to extend the −3dB bandwidth at the cost of a small peak in the amplitude response.

The improvement is shown by calculating the frequency with the compensating coil:

$$f_{comp} = \frac{2{\cdot}22}{1{\cdot}59}.f = 1{\cdot}4f \simeq 4{\cdot}2\text{MHz}.$$

The value of the compensating inductor would be:

$$L = \frac{0{\cdot}5 \times 13 \times 3{\cdot}9^2 \times 10^6}{10^{12}} \simeq 100\mu\text{H}.$$

The bandwidth may be further extended by partial decoupling of the emitter resistor. The value of capacitor required is determined by the consideration that the emitter and collector network time-constants should be approximately equal.

**Stage Gain and D.C. Stability**

The low-frequency stage gain is determined closely by the ratio of collector load resistance to emitter resistance. Typically, gains of 20 to 30 times are required, corresponding to emitter resistances between 195Ω and 130Ω (with 3·9kΩ collector load resistance).

If a transistor is connected in series with the emitter resistor for flyback blanking, its bottomed resistance will be typically about 20Ω (BC148) therefore the emitter resistor value must be lower by that amount to achieve the desired gain.

To enable the BF178 to be used to its maximum capabilities it is essential, for satisfactory d.c. stability, that the emitter network resistance is not less than 100Ω and the total base network d.c. resistance is not greater than 1kΩ. Because of the practical necessity of driving a video transistor from a low source resistance these conditions are easily met.

**Input Impedance of Video Transistor**

Video transistors have an appreciable input capacitance, and this chiefly determines the requirements for the previous stage.

At low frequencies (below 5MHz) the input impedance of a video stage having a partly decoupled emitter resistor is equivalent to a resistance and capacitance in parallel having the approximate values:

$$R_{in} = h_{FE} R_E \qquad \ldots(1)$$

and

$$C_{in} = \frac{C_E}{h_{FE}} + \frac{1}{2\pi f_T R_E} + (A+1).c_{re} \qquad \ldots(2)$$

where

$h_{FE}$ = current transfer ratio
$R_E$ = emitter resistance
$C_E$ = emitter compensating capacitance
$f_T$ = transition frequency
$A$ = stage voltage gain
$c_{re}$ = feedback capacitance.

In Eqs. 1 and 2, we may now insert the following values

$R_E = 150\Omega$
$C_E = 220\text{pF}$
$h_{FE} = 20$
$f_T = 120\text{MHz}$
$A = 25$
$c_{re} = 2{\cdot}5\text{pF}.$

Then,

$$R_{in} = 20 \times 150 = 3\text{k}\Omega$$

$$C_{in} = \frac{220}{20} + \frac{10^{12}}{2\pi \times 120 \times 10^6 \times 150} + 26 \times 2{\cdot}5(\text{pF})$$
$$= 11 + 8{\cdot}8 + 65$$
$$\simeq 85\text{pF}.$$

The major contribution to the input capacitance is evidently due to the Miller effect.

It is clearly not practicable to drive directly from the video detector therefore an intermediate impedance matching stage is required. This is now described.

## VIDEO DRIVER STAGE

**Output Resistance**

The output resistance of the matching stage together with the input resistance and capacitance of the video transistor form a network whose time-constant should be compatible with the required bandwidth.

If we assume a −3dB point at 5MHz, and $C_{in} \simeq 85\text{pF}$:

$$R_{tot} \leqslant \frac{10^{12}}{2\pi \times 5 \times 10^6 \times 85} \simeq 380\Omega.$$

Therefore, ideally, ignoring $R_{in}$, the output resistance of the driver stage should not exceed this value. However, in most practical cases a value of 500Ω can be used because of the increase in bandwidth available by means of partial decoupling of the emitter of the output transistor with a low value capacitor.

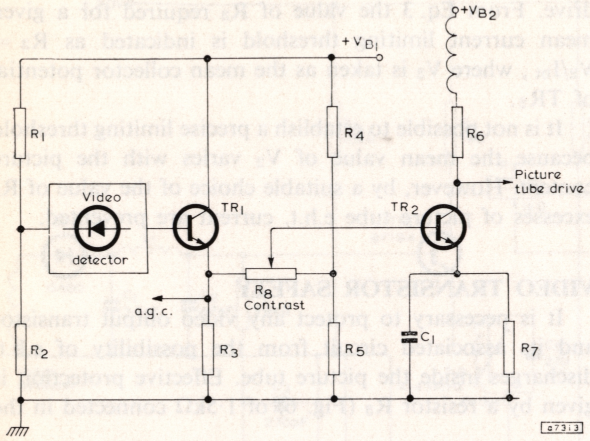

Fig. 2—Constant black level contrast control with emitter follower

The matching stage can be connected to supply the video output transistor from either its emitter (emitter follower, Fig. 2) or from its collector (phase splitter, Fig. 3). In the case of the emitter follower, its output resistance is very low during transients when the emitter current is rising: but when its current is falling rapidly its output resistance is equal to that of its emitter network resistance. In the case of the phase splitter the output resistance at the collector is practically equal to the collector network resistance whether the transistor current is rising or falling. In either case, therefore, the load resistance should not be greater than 500Ω.

**Video Detector Loading**

Eqs. 1 and 2 can be used to obtain the input resistance and capacitance of the video driver stage.

If a BF184 having values of $h_{FE} = 75$, $f_T = 300\text{MHz}$, $c_{re} = 0{\cdot}65\text{pF}$ is employed as an emitter follower with $R_E = 470\Omega$, $C_E = 85\text{pF}$ and $A = 0$, the equivalent parallel values of input impedance are as follows.

$$R_{in} = 75 \times 470 \simeq 35\text{k}\Omega$$

$$C_{in} = \frac{85}{75} + \frac{10^{12}}{2\pi \times 300 \times 10^6 \times 470} + 0{\cdot}65$$
$$= 1{\cdot}15 + 1{\cdot}15 + 0{\cdot}65$$
$$\simeq 3\text{pF}.$$

In the case of a video splitter stage $C_{in}$ will be slightly higher because A appears in the equation. However, in either case the input impedance of the driver stage is acceptable to a video detector circuit having a 3·9kΩ load resistance.

## CONTRAST CONTROL METHODS

**Base Network Control**

A contrast control technique which maintains a constant black level is shown for the emitter follower in Fig. 2. The d.c. level and amplitude of the video signal at the emitter of $TR_1$ are defined by $R_1$, $R_2$ and by the a.g.c. system. If the values of $R_4$ and $R_5$ are chosen to give a voltage of $V_1$ equal to the black level of the video signal at the emitter of $TR_1$, the black level of the signal fed to $TR_2$ will remain constant over the contrast control range. Because of bandwidth considerations, $R_8$ should not be higher in value than 1kΩ. The parallel value of $R_4$ and $R_5$ should be about one quarter the value of $R_8$ thus giving a contrast range of about 5:1.

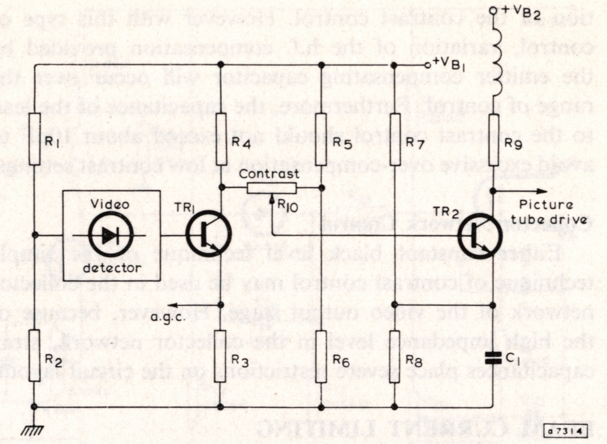

Fig. 3—Constant black level contrast control with phase splitter

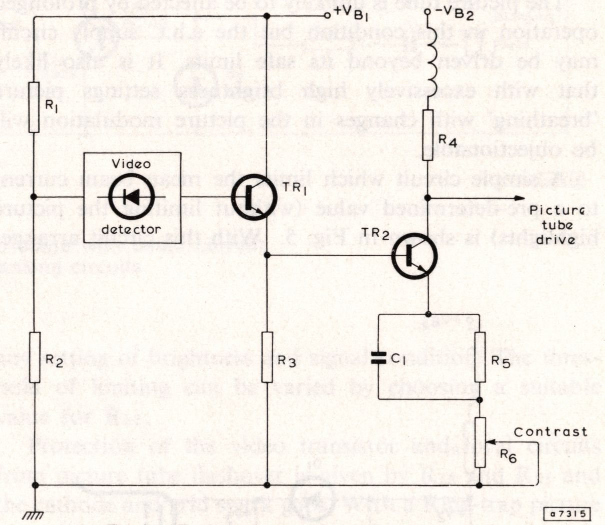

Fig. 4—Emitter network contrast control

The same technique can be applied to the phase splitter driver stage as shown in Fig. 3. It is necessary, however, to elevate the emitter of the video output transistor $TR_2$ to about 1V less than the black level of the signal from the contrast control. The values of $R_7$ and $R_8$ in parallel should provide the desired value of emitter resistance for $TR_2$.

**Emitter Network Control**

A contrast control technique by variation of the emitter resistance of the video output stage is shown in Fig. 4. This has the merit of simplicity but it does not maintain a constant black level. A potentiometer having a suitable inverse law would be required to avoid non-linear operation of the contrast control. However with this type of control, variation of the h.f. compensation provided by the emitter compensating capacitor will occur over the range of control. Furthermore, the capacitance of the lead to the contrast control should not exceed about 10pF to avoid excessive over-compensation at low contrast settings.

**Collector Network Control**

Either constant black level technique or the simple technique of contrast control may be used in the collector network of the video output stage. However, because of the high impedance level in the collector network, stray capacitances place severe restrictions on the circuit layout.

## BEAM CURRENT LIMITING

In a d.c. coupled video stage in a negative modulation system the picture tube can be driven to a high brightness level if the input signal is removed.

The picture tube is unlikely to be affected by prolonged operation in this condition but the e.h.t. supply circuit may be driven beyond its safe limits. It is also likely that with excessively high brightness settings picture 'breathing' with changes in the picture modulation will be objectionable.

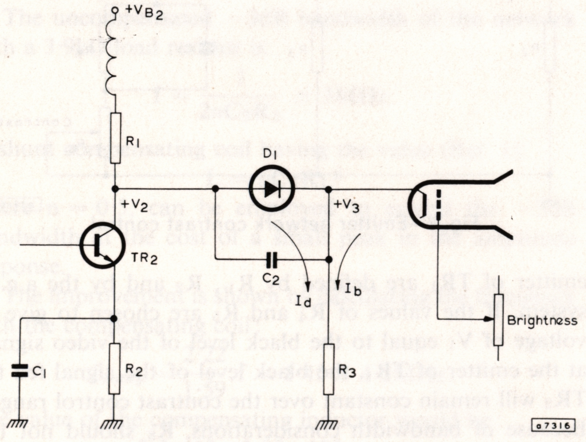

Fig. 5—Simple beam current limiting circuit

A simple circuit which limits the mean beam current to a pre-determined value (without limiting the picture highlights) is shown in Fig. 5. With this circuit arrangement, d.c. coupling is maintained only on low key scenes, where it is most important. In this circuit,

$$V_3 = (I_d+I_b)R_3 = I_dR_3+I_bR_3.$$

The diode will remain conducting and clamp the picture tube cathode to the collector of the video transistor $TR_2$ as long as $I_bR_3 < V_2$. At the threshold of limiting,

$$I_{bt}R_3 = V_2 = V_3. \qquad \ldots(3)$$

Therefore,

$$I_d = 0.$$

Beyond this threshold $V_2 < V_3$ and the capacitor $C_2$ charges to $V_3-V_2$, that is, the picture tube drive is now a.c. coupled. The picture tube therefore receives an additional back-bias proportional to the excess mean drive. From Eq. 3 the value of $R_3$ required for a given mean current limiting threshold is indicated as $R_3 = V_2/I_{bt}$, where $V_2$ is taken as the mean collector potential of $TR_2$.

It is not possible to establish a precise limiting threshold because the mean value of $V_2$ varies with the picture content. However, by a suitable choice of the value of $R_3$ excesses of picture tube e.h.t. current are prevented.

## VIDEO TRANSISTOR SAFETY

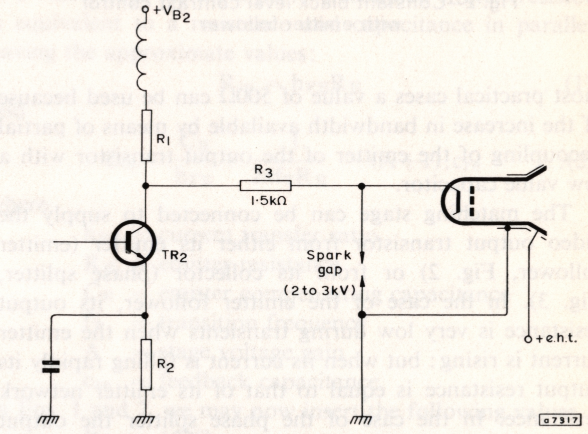

Fig. 6—Protection of video transistor from picture tube flashover

It is necessary to protect any video output transistor and its associated circuit from the possibility of e.h.t. discharges inside the picture tube. Effective protection is given by a resistor $R_3$ (Fig. 6) of 1·5kΩ connected in the cathode lead of the picture tube together with a spark gap which breaks down at about 2 to 3kV (Ref. 2). It is essential to connect the earthy end of the spark gap to the picture tube aquadag by a low inductance lead and to earth the aquadag at the earthy end of the spark gap. This will ensure that flashover currents are returned directly to the picture tube without passing through the chassis and circuit wiring.

During the receiver warm-up period the h.t. rail to the video stage can be permitted to rise above the rated maximum $V_{CER}$ for a limited duration (BF178 data).

## CIRCUIT DESCRIPTION AND PERFORMANCE

**Full Performance Circuit**

A practical circuit of a complete video stage is shown in Fig. 7. It is driven from a phase splitter and incorporates a constant black level contrast control together with beam current limiting and flyback blanking circuits. The video output stage operates from a +250V line with a split collector load giving an effective load resistance value of approximately 3·9kΩ, from a source of +150V.

The video detector supplies a positively-detected signal (positive-going sync) to the video splitter, $TR_1$, which is biased with a small positive set-up voltage ($R_2$, $R_3$) to avoid the compression of peak whites in the transistor. The signal at the emitter is fed to the a.g.c. system (sync tip level) and the sync pulse separator via $R_6$. With an emitter resistor ($R_5$) of 470Ω and a collector network resistance of approximately 500Ω the gain of the splitter stage is approximately unity. The a.g.c. threshold is adjusted to set the sync tip level at the base of $TR_1$ to +6·5V and this gives a signal black level potential at the collector of $TR_1$ of +10V. A corresponding potential of +10V is supplied by $R_8$ and $R_9$ for the low level end of the contrast control.

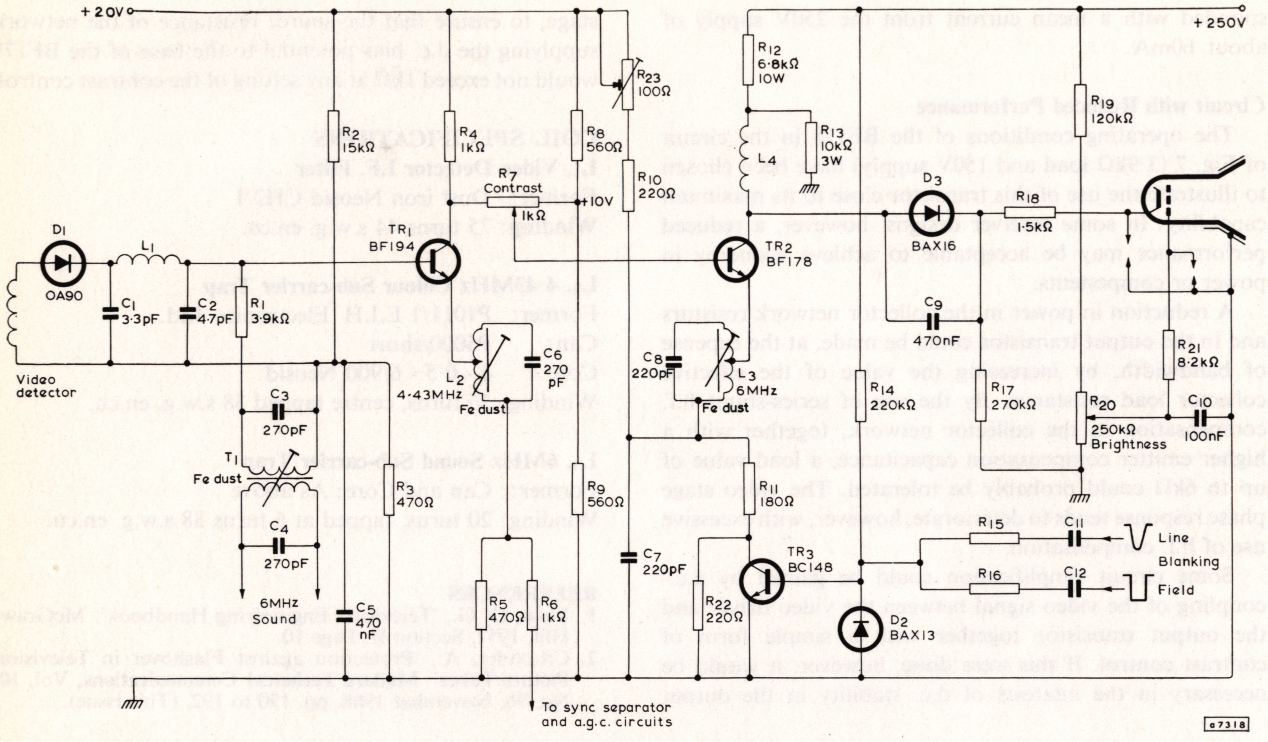

Fig. 7—Example of complete video stage with beam current limiting and flyback blanking circuits

The emitter potential of the video stage $TR_2$ is also elevated to about +9V by $R_{10}$, $R_{11}$ and $R_{23}$, the latter being adjusted to set the black level potential at the collector of $TR_2$ to about +130V. The gain of the video stage is approximately 25 times.

The flyback blanking transistor $TR_3$ is held in conduction by the base current supplied by $R_{14}$. Negative-going line and field timebase flyback pulses are added via $R_{15}$ and $R_{16}$, and are applied to the base of $TR_3$. During the flyback period the video stage is thus cut off, with the collector of $TR_2$ at approximately +150V, about 20V higher than the picture tube drive black level. Diode $D_2$ limits the negative potential on the base of $TR_3$ due to the charge gained by the coupling capacitors $C_{11}$, $C_{12}$, and also promotes adequate clipping of the input waveform. $R_{22}$ is connected across $TR_3$ to prevent the emitter of $TR_2$ rising towards the positive l.t. line potential during the blanking pulses.

Without the picture tube beam current limiting components $C_9$, $R_{17}$ and $D_3$ the mean beam current could exceed 2mA with maximum brightness setting and with the input signal removed. The limiting circuit effectively prevents the beam current rising above about 400μA with any setting of brightness and signal condition. The threshold of limiting can be varied by choosing a suitable value for $R_{17}$.

Protection of the video transistor and local circuits from picture tube flashover is given by $R_{18}$ and $R_{21}$ and the cathode and grid spark gaps. With a Ring-trap picture tube the separate spark gaps are, of course, unnecessary. The sum of $R_{18}$ (1·5kΩ) and $R_{21}$ (8·2kΩ) make up the 10kΩ (approximately) total series resistance in the picture tube grid and cathode network, the purpose of which is to limit the magnitude of grid current, as specified by the published data.

## PERFORMANCE

The −3dB bandwidth of the collector network of the video transistor with the picture tube connected and without the shunt compensating inductor $L_4$ was 4MHz. The insertion of $L_4$ (100μH) extended this to about 5·7MHz. The −3dB bandwidth of the complete stage from the base of $TR_1$ to the collector of $TR_2$, without the two emitter trap networks in circuit, and without the emitter compensation capacitor $C_7$ connected, was about 4·5MHz at maximum contrast and about 5·5MHz at minimum contrast. These figures increased to at least 6·5MHz when the emitter compensation capacitor $C_7$ was connected. The traps $L_2$, $C_6$ and $L_3$, $C_8$ give adequate rejection at the colour subcarrier and sound carrier frequencies respectively.

The available video output amplitude was in excess of 100V black-to-white at maximum contrast. This corresponded with a mean current from the 250V supply of about 60mA.

### Circuit with Reduced Performance

The operating conditions of the BF178 in the circuit of Fig. 7 (3·9kΩ load and 150V supply) have been chosen to illustrate the use of this transistor close to its maximum capability. In some receiver designs, however, a reduced performance may be acceptable to achieve economy in power or components.

A reduction in power in the collector network resistors and in the output transistor could be made, at the expense of bandwidth, by increasing the value of the effective collector load resistance. By the use of series-shunt h.f. compensation in the collector network, together with a higher emitter compensation capacitance, a load value of up to 6kΩ could probably be tolerated. The video stage phase response tends to deteriorate, however, with excessive use of h.f. compensation.

Some circuit simplification could be gained by a.c.-coupling of the video signal between the video driver and the output transistor together with a simple form of contrast control. If this were done, however, it would be necessary in the interests of d.c. stability in the output stage, to ensure that the source resistance of the network supplying the d.c. bias potential to the base of the BF178 would not exceed 1kΩ at any setting of the contrast control.

## COIL SPECIFICATIONS

### $L_1$, Video Detector I.F. Filter

Former: Dust iron Neosid CH2/1
Winding: 75 turns 44 s.w.g. en.cu.

### $L_2$, 4·43MHz Colour Sub-carrier Trap

Former: P1011/1 E.I.H Electronics Ltd.
Can: P5000/short
Core: 4×0·5×6/900 Neosid
Winding: 36 turns, centre tapped 38 s.w.g. en.cu.

### $L_3$, 6MHz Sound Sub-carrier Trap

Former: Can and Core: As above
Winding: 20 turns, tapped at 6 turns 38 s.w.g. en.cu.

## REFERENCES

1. Fink, D. G., 'Television Engineering Handbook'. McGraw-Hill, 1957, Section II, Page 10.
2. Ciuciura, A., 'Protection against Flashover in Television Picture Tubes' **Mullard Technical Communications,** Vol. 10, No. 96, November 1968, pp. 190 to 192. (This issue).